# EVALUATION OF LONGITUDINAL JOINTS OF HMA PAVEMENTS IN TENNESSEE

Submitted to the Tennessee Department of Transportation

Research Development and Technology Program

Project #: _ RES 1304

**Baoshan Huang, Ph.D., P.E.**

**Xiang Shu, Ph.D.**

**Department of Civil and Environmental Engineering**

**The University of Tennessee, Knoxville**

**May 2010**

## Technical Report Documentation Page

| 1. Report # | 2. Government Accession # | 3. Recipient's Catalog # |
|---|---|---|

| 4. Title & Subtitle | 5. Report Date |
|---|---|
| Evaluation of Longitudinal Joints of HMA Pavements in Tennessee | May 2010 |
| **7. Author(s)**<br>Baoshan Huang and Xiang Shu | **6. Performing Organization Code** |
| **9. Performing Organization Name & Address**<br>Depart of Civil and Environmental Engineering<br>The University of Tennessee<br>223 Perkins Hall<br>Knoxville, TN 37996 | **8. Performing Organization Report #**<br><br>**10. Work Unit # (TRAIS)** |
| **12. Sponsoring Agency Name & Address**<br>Tennessee Department of Transportation<br>James K. Polk Building, Suite 700<br>505 Deaderick Street<br>Nashville, TN 37243-0349 | **11. Contract or Grant #**<br>TDOT Research #: RES 1304<br><br>**13. Type of Report & Period Covered**<br>Final Report 2007-2010<br><br>**14. Sponsoring Agency Code** |

**15. Supplementary Notes**

**16. Abstract**

Longitudinal joints between lanes of hot-mix asphalt (HMA) pavements are commonly susceptible to moisture damage and other failures. In 2006, the Tennessee Department of Transportation (TDOT) identified longitudinal joint failure as one of the major distresses for local HMA pavements. It was determined necessary to evaluate available practices and technologies to reduce longitudinal joint failure.

This study presents the results from three field projects in Tennessee constructed with seven different longitudinal joint construction techniques. These techniques could be divided into three major categories: joint adhesives (Crafco, Pavon, polymer emulsion and basic emulsion commonly used by TDOT), joint sealers (Jointbond and Replay), and infrared joint heater. Laboratory tests were conducted on the field cores taken from the test sections constructed with different techniques. The laboratory tests included air void content, permeability, indirect tensile (IDT) strength, water absorption, and X-ray CT tests.

The results from the laboratory tests show general consistency in characterizing the longitudinal joint construction quality, i.e., the lower the air void content, the lower the permeability, and the higher the IDT strength. Without any special treatment, longitudinal joint exhibited the lowest construction quality, followed by the mat on the cold side. Among the joint adhesives, polymer emulsion appeared to increase the IDT strength of joint. The results from water absorption test indicate that joint sealers may be effective in improving joint performance by preventing water from penetrating into pavement joint. The infrared heater exhibited the best effectiveness in improving joint quality among all the joint construction techniques used in this study.

| 17. Key Words | 18. Distribution Statement |
|---|---|
| Asphalt pavement, longitudinal joint, construction, joint adhesive, joint seal, infrared heating, air voids, permeability, strength, water absorption, X-ray CT | No restrictions. This document is available to the public through the National Technical Information Service, Springfield, VA 22161 |

| Security Classification (of this report) | Security Classification (of this page) | 21. # Of Pages | 22. Price |
|---|---|---|---|
| Unclassified | Unclassified | 88 | |

Form DOT F 1700.7 (5-02) Reproduction of completed page authorized

# Acknowledgements

We would like to begin by thanking the Tennessee Department of Transportation (TDOT) for funding this research project. During this research, we have collaborated closely with engineers and technicians at the TDOT Materials and Test Division. They have provided valuable support towards the fulfillment of the research objectives. Without their support, it would be impossible for us to finish this research project. We would also like to thank the administrative staff from the TDOT research office who have worked very closely with our research team and kept the whole project on the proposed schedule. Thanks also go to the Tennessee Road Builders Association (TRBA) for coordinating the selection of the joint products for the study.

# Table of Contents

# CHAPTER 1 INTRODUCTION

## 1.1 Problem Statement

Longitudinal joints between lanes of hot-mix asphalt (HMA) pavements are commonly susceptible to moisture and other failures. Like many other states, HMA paving in Tennessee almost exclusively adopts the practice of paving one lane at a time. Hence there is commonly the problem of compacting hot-mix asphalt adjacent to existing cold HMA lane(s). Several factors have beemn identified to be the causes of HMA joint failures. First, it is difficult to achieve the desired pavement densities near the longitudinal joints with normal compaction techniques. Lower densities mean higher air voids and lower pavement strength, which will likely introduce moistures into the open voids and cause pavement failures. Secondly, interface bond between existing cold HMA pavement lane(s) and newly constructed lane(s) can never achieve the strength of HMA inherent strength (cohesion) without joint treatments. In addition, the orientations of longitudinal joints are usually in-line with wheel loads, which result in maximum shear stress on the weakly bonded interface.

Over the years, longitudinal joint failure has been one of the major distresses for pavements in Tennessee. It is necessary to evaluate the available practices and technologies and find the best solutions that will mitigate and/or eliminate longitudinal failures for HMA pavements in Tennessee.

## 1.2 Objectives

The objectives of the proposed research are

(1) to investigate the fundamental mechanisms of longitudinal joint failure for HMA pavements in Tennessee;

(2) to evaluate several available technologies and construction practices that will mitigate HMA longitudinal failures; and

(3) to recommend the necessary changes to the current TDOT specifications that will ensure the quality of longitudinal joints for HMA pavements in Tennessee.

## 1.3 Scope of Study

The scope of the research work includes:

- To complete a synthesis of literature review and DOT surveys on the construction methods of longitudinal joints of HMA pavements in US;
- To select several test sections (each 500 feet long) of HMA pavement constructed using different longitudinal joint construction techniques and evaluate the performance of these longitudinal joints.
- The longitudinal joint construction techniques include, the conventional method (as control), rolling from hot side 6 inch away from joint, notched wedge joint, cutting wheel, heating joints, joint maker, restrained edge, and any others that may be selected. In addition, joint adhesives or tapes may or may not be used in the longitudinal joints.
- Field tests, including nuclear density test and permeability/vacuum test, will be conducted over the longitudinal joints and at some locations away from longitudinal joints at the pre-specified intervals.
- Cores will be taken from the longitudinal joints and other locations away from longitudinal joints (same as field tests) at the pre-specified intervals for laboratory testing. Laboratory tests include density and direct shear tests.
- Field visual evaluation of longitudinal joints will be performed annually after construction.

# CHAPTER 2 LITERATURE REVIEW

## 2.1 Background

Longitudinal joints widely exist between adjacent lanes of hot-mix asphalt (HMA) pavements. Improperly constructed longitudinal joints are potentially susceptible to premature deterioration in the form of cracking and/or raveling due to the relatively high air void content. High air void content (or low density) is common for longitudinal joints constructed with normal compaction techniques since the edge of the first paved lane (cold lane) is unconfined. As the roller passes over, this unconfined edge tends to deform laterally rather than compact. The subsequent lane (hot lane) is confined by the previously paved lane and therefore can be more densely compacted. The overall air void content of longitudinal joints is still higher than pavements away from the joints. Usually, a well-constructed longitudinal joint is about 1-2 percent lower in density than the rest of the lane away from the joint; however a poorly-constructed longitudinal joint can have significantly low density – on the order of 5-10 percent (Foster et al., 1964; Livneh, 1988; Burati and Elzoghbi, 1987; Kandall and Mallick, 1996). Burati and Elzoghbi (1987) studied joint densities in asphalt pavements of two airports and found that joint core densities were significantly lower than mat core densities at both airports. Estakhri et al. (2002) evaluated 35 highway pavements in Texas and found that the density was always lower at the unconfined edge than in the middle of the lane and this was almost always statistically significant.

The high air voids in the longitudinal joints allows water infiltration into HMA pavements and accelerates the aging process of asphalt binder, which eventually leads to the premature distresses, usually in the form of longitudinal cracking. Sometimes, cracks develop along longitudinal joints within one year of service.

Currently, various construction techniques, equipment, devices, and products are available to improve the quality of longitudinal joints and reduce the risk of longitudinal cracking. The following provides a brief literature review on the studies to evaluate the effectiveness of different joint construction techniques in improving the longitudinal joint performance.

## 2.2 Longitudinal Joint Study at NCAT

Since 1992, the National Center of Aspahtl Technology (NCAT) has conducted an extensive study on longitudinal joints (Kandhal and Rao 1994a,b; Kandhal and Mallick 1996a,b, 1997a,b, 2007; Buchanan 2000; Kandhal et al. 2002). They evaluated various longitudinal joint construction techniques for HMA pavements in several states of the United States (Michigan, Wisconsin, Colorado, Pennsylvania, and New Jersey). The following longitudinal joint construction techniques were evaluated by the NCAT:

- **Notched Wedge Joint:** A steel plate or special device attached to the paver screed is used to form the notched wedge joint by providing a vertical notch and a taper (vertical: horizontal =1;12) at the edge of the first-paved lane.
- **Edge Restraining Device:** It is a hydraulically powered wheel that rolls alongside the compaction drum and thus provides the restraint at the edge of the first-constructed lane during compaction.
- **Cutting Wheel:** It is a 10-inch (254-mm) diameter cutting wheel mounted on an intermediate roller and used to cut 1½-2 inches (38-51 mm) of the unconfined, low-density edge of the first lane after compaction, while the mix is still plastic.
- **Joint Maker:** This is a boot-like device attached to the side of the screed at the corner during construction. The device forces extra material at the joint through an extrusion process prior to the screed.
- **Tapered (1:3) Joint with Vertical One-Inch Offset:** This joint consists of a 1-inch (25 mm) vertical step (offset) at the top of the joint and a 1:3 taper starting from the

base of the vertical step.

- **Rubberized Asphalt Tack Coat:** A tack coat is applied to edge of the cold lane before paving the hot side.
- **New Jersey Wedge (1:3):** This 1:3 tape wedge joint is formed during construction of the first lane by using a sloping steel plate attached to the inside corner of the paver screed extension.

In addition, three different joint rolling patterns were also included in the NCAT study. The three rolling patterns are:

- **Rolling from Hot Side**: Compaction is done from the hot side with a 6-inch overlap on the cold lane.
- **Rolling from Cold side**: Compact starts from the cold side with a 6-inch overlap on the hot lane.
- **Rolling from Hot Side 6 Inch Away from Joint**: Compaction starts with the roller edge approximately 6-inches away from the joint on the hot side.

Field cores were taken from the test sections to test in the laboratory for their density and air voids. The joint performance was inspected by a team of engineers at least once a year after construction. Based on the statistical analysis of test results and field visual performance evaluation, the following conclusions and recommendations were drawn from the NCAT study (Kandhal and Rao 1994a,b; Kandhal and Mallick 1996a,b, 1997a,b, 2007; Buchanan 2000; Kandhal et al. 2002):

1. Rubberized asphalt tack coat gives the best joint performance with no significant cracking, closely followed by cutting wheel.
2. The notched wedge joint with 1:12 taper shows the best potential of a satisfactory longitudinal joint performance. The vertical offset is considered very essential to joint performance.
3. The cutting wheel and the edge-restraining devices can produce good joint quality. But they are highly operator dependent and may not always give consistent

performance results.

4. Rolling the longitudinal joint from the hot side 150 mm (6 inch) away from the joint for the first roller pass is observed to be the best compaction method.
5. NCAT recommended that the minimum acceptable compaction level be specified, which should be no more than two percent lower in density than the density specified for the mat away from the joint.
6. NCAT also recommended that the density of longitudinal joint be determined by taking cores, rather than using nuclear density gage because of the seating problem on the joint.

## 2.3 Longitudinal Joint Study at Kentucky Transportation Center

A comprehensive longitudinal joint study was undertaken by the Kentucky Transportation Center in 1999 to evaluate different longitudinal joint construction methods (Fleckenstein et al., 2002). 12 construction projects were included in the study. Each project included a test section in which special joint construction technique was adopted and a control section. On some of the projects, more than one technique was used. The following joint construction techniques were evaluated:

- Notched Wedge Joint
- Restrained Wedge
- Joint Maker
- Infrared Joint Reheater
- Joint Adhesives

After compaction, nuclear density test and permeability/vacuum test were performed and field cores were taken at the centerline of the joint and its neighboring area for each project.

The major conclusions and recommendations from this study include:

1. Without any special joint construction technique or compactive effort, the density at or near the construction joint can be achieved to be within three percent of the lane density. This can be used as a basis for future specification.
2. The infrared joint reheater achieved the highest joint density among all the joint construction techniques.
3. The restrained-wedge achieved the second highest overall density and was significantly better than the conventional construction method.
4. The notched wedge joint gave the third highest overall density and only marginally improved the joint construction quality.
5. The joint maker did not show any improvement over conventional construction technique.
6. The notched-wedge joint appeared to produce the lowest permeability at the joint.
7. Preliminary performance data indicate that the projects with joint adhesives perform as well as or better than projects without joint adhesives.

## 2.4 Longitudinal Joint Study at Wisconsin Department of Transportation

In 1993, the Wisconsin Department of Transportation initiated a study to accompany the NCAT longitudinal joint study due to the difference in wedge joint performance in NCAT study and in Wisconsin (Toepel 2003). Unlike in the NCAT study, the wedge joint did not perform well in the Wisconsin project. The Wisconsin wedge joint did not include a vertical offset of ½ inch at the top of the wedge and was constructed differently from it was in Michigan due to lack of experience and proper equipment.

In this study, eight longitudinal joint construction techniques were evaluated with a focus on the wedge joint. They are:

- Conventional Method

- Wedge Joint with Truck Tire Rolling
- Wedge Joint without Rolling
- Wedge Joint with Steel Side Roller Wheel
- Wedge Joint with Rubber Side Roller Wheel
- Wedge Joint with Tag-along Roller,
- Cut Joint Method
- Edge Restraining Method

Joint performance was evaluated based on density results and an overall performance ranking based on amount of longitudinal joint cracking. The following conclusions and recommendations were drawn from the study:

1. The wedge joint performed better than the cut joint and the restrained edge joint. when constructed with better equipment and by more experienced workers, the wedge joint in Wisconsin performs as well as it does in Michigan;
2. From the constructability standpoint, the wedge joint creates less debris and can be constructed more efficiently than the cut wheel joint and the restrained edge joint.
3. The wedge joint constructed by steel side roller wheel and the wedge joint constructed by tag-along roller perform the best. However, it is much easier to construct the wedge joint with the steel side roller wheel than with the tag-along roller because the paver operator is difficult to see the tag-along roller.

# CHAPTER 3 RESEARCH METHODOLOGY

## 3.1 Description of Field Projects

### 3.1.1 Project CNF923

The Project CNF923 is a two-lane resurface project constructed on Highway 160 and started from Exit 12 of Interstate 81 near Morristown, TN (Figure 3-1). The west bound lane was paved first. Joint heating technique was adopted when the east bound lane was paved on October 31, 2007. The heating equipment used for this project was a propane fired joint heater manufactured by Heat Design Equipment Inc. The joint heater can be towed along the paving joint and continuous paving can be obtained. The type of joint heater used in the project is HDE JMH 400T, which has a heating deck 16 feet long by 18 inches wide (Figure 3-2). The deck consists of four individual heaters, each four feet long, with a heating output of up to 112, 000 Btu per hour (Figure 3-3). The heater employs multiple layers of a patented ceramic and steel fabric to generate true infrared heat which reheats asphalt mixes to 2.5 inches in depth without damage or change to asphalt mix. The temperature was determined to be 270°F (132 °C) immediately after heated.


Figure 3-1 Location of Project CNF923


Figure 3-2 Heating Equipment (HDE JMH 400T)


Figure 3-3 Infrared Heater

Field cores were taken twice from the Project CNF923. Coring locations and pattern are shown in Figures 3-4 and 3-5. Seven cores (cores No. 3-5 and 8-11) were taken after compaction at one location for the first time on the same day of construction, Oct. 31, 2007. On Feb. 14, 2008, field cores were taken for the second time at three different locations (Figure 3-4). At each location, 11 cores were taken in the manner shown in Figure 3-5. Figure 3-6 shows the positions of field cores at one location before and after coring. Figure 3-7 shows the coring operation by TDOT engineers. Figure 3-8 shows the cores taken from the longitudinal joint and the neighboring area.

Each core is 6 inches in diameter and about 4.5 inches high. The cores were transported to the Infrastructure Materials Lab at the University of Tennessee for laboratory testing. For this project, the laboratory testing includes air voids test, water permeability test, and indirect tensile strength test. The mix design of the HMA mixture used in this project is shown in Table 3-1.

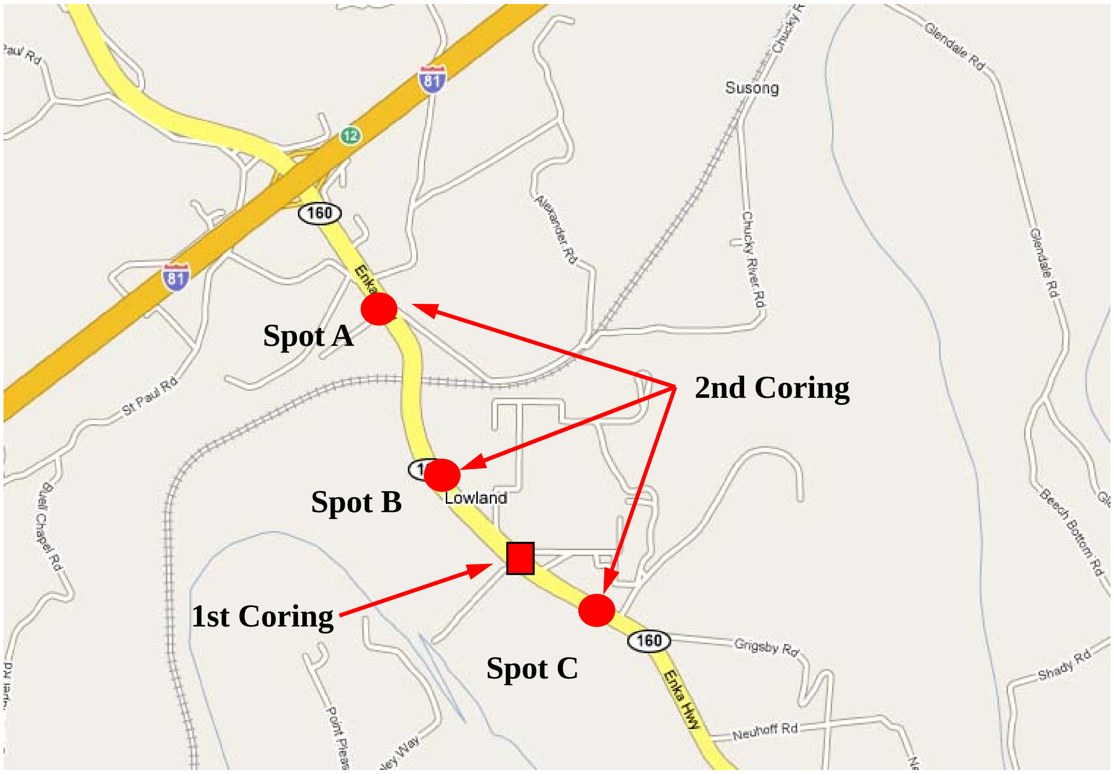


Figure 3-4 Coring Locations

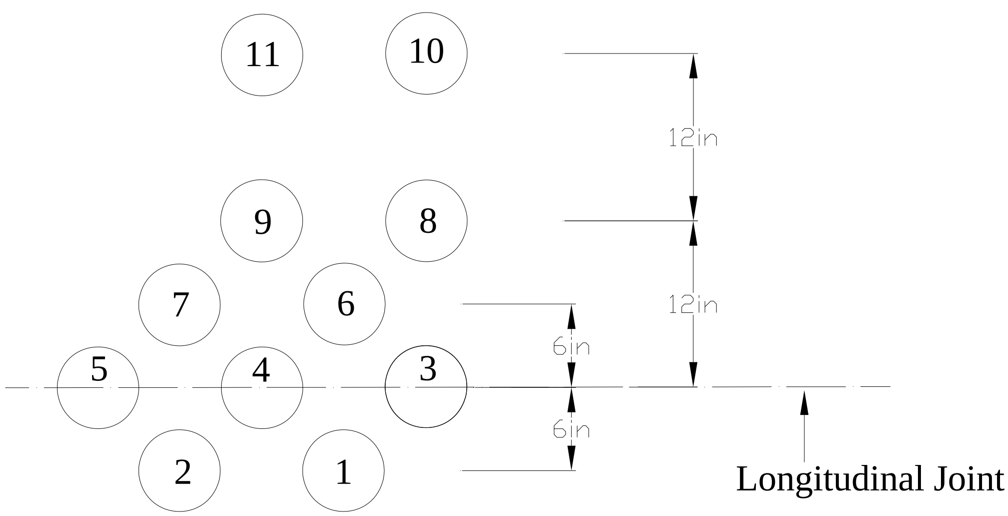


Figure 3-5 Coring Pattern (Note: Only seven cores, i.e., cores No. 3-5 and 8-11 were taken for the first time.)


(a) Before Coring


(b) After Coring

Figure 3-6 Core Positions at One Coring Location

Figure 3-7 Field Coring

Figure 3-8 Field Cores

Table 3-1 Mix Proportion for Project CNF923

| **Aggregate Composition** | | |
|---|---|---|
| Percent Used | Source | |
| 50 | D Rock (Gravel), Vulcan Mtls Chucky, TN | |
| 10 | #10 Screenings (Soft), Vulcan Mtls Greeneville, TN | |
| 25 | Natural sand, Vulcan Mtls Chucky, TN | |
| 15 | RAP, Summers Taylor Matls Greeneville, TN | |
| **Blend Gradation** | | |
| Sieve | Percent Passing | |
| 16 mm (5/8″) | 100 | |
| 12.5 mm (1/2″) | 96 | |
| 9.5 mm (3/8″) | 85 | |
| 4.75 mm (No.4) | 58 | |
| 2.36 mm (No.8) | 40 | |
| 0.6 mm (No.30) | 20 | |
| 0.3 mm (No.50) | 12 | |
| 0.15 mm (No.100) | 6.2 | |
| 0.075 mm (No.200) | 3.6 | |
| **Mix Design Information** | | |
| Optimum Asphalt Content (%) | 5.7 | |
| AC Grade | PG 64-22 | |
| Mixing Temperature (°F) | 290-320 | |
| Tensile Strength Ratio (%) | 91.6 | |

### 3.1.2 Project CNG072

The Project CNG072 was a resurfacing on the US 25W (SR 9) from SR 63 to west of Jane Way Lane in La Follette, Tennessee. It was constructed with the conventional construction method, i.e., no special joint construction technique was adopted for this project.

Field cores were taken at three different locations, Spots A, B, and C (Figure 3-9) on May 20, 2008, a few days after construction. Spot A is on the longitudinal joint of two west bound lanes, while Spots B and C are on the longitudinal joint of two east bound lanes. At each location, 16 cores were taken in the manner shown in Figure 3-10. Figure

3-11 shows the coring positions at one location before and after coring. Figure 3-12 shows the coring operation by TDOT engineers. Figure 3-13 shows the cores taken at one location. The cores were 6 inches in diameter and varied in thickness.

Totally, 48 cores were taken and transported to the Infrastructure Materials Lab at the University of Tennessee for laboratory testing. For this project, the laboratory testing includes air voids test, water permeability test, and indirect tensile strength test.

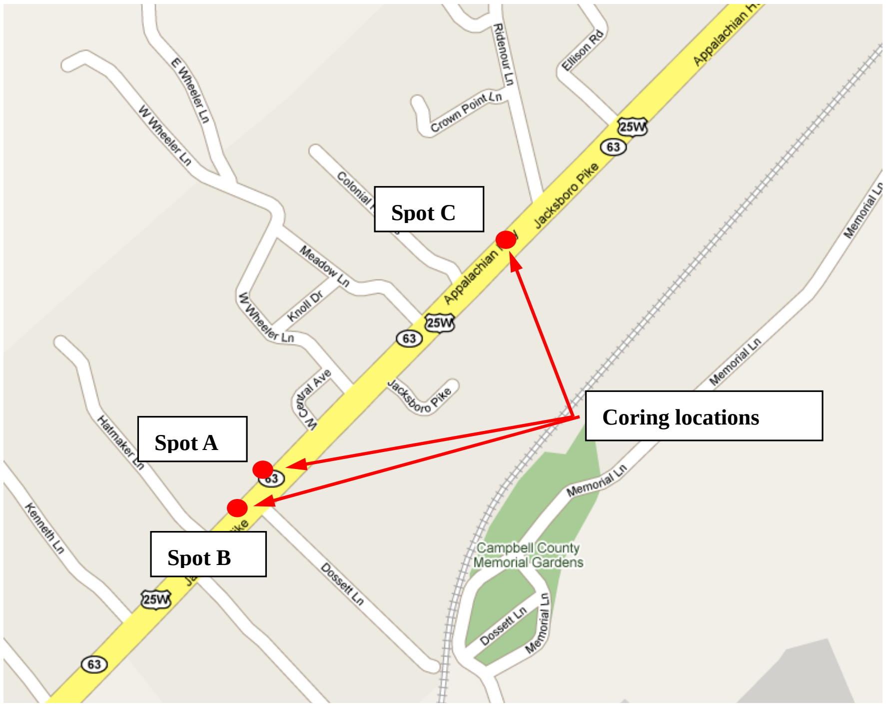


Figure 3-9 Coring Locations

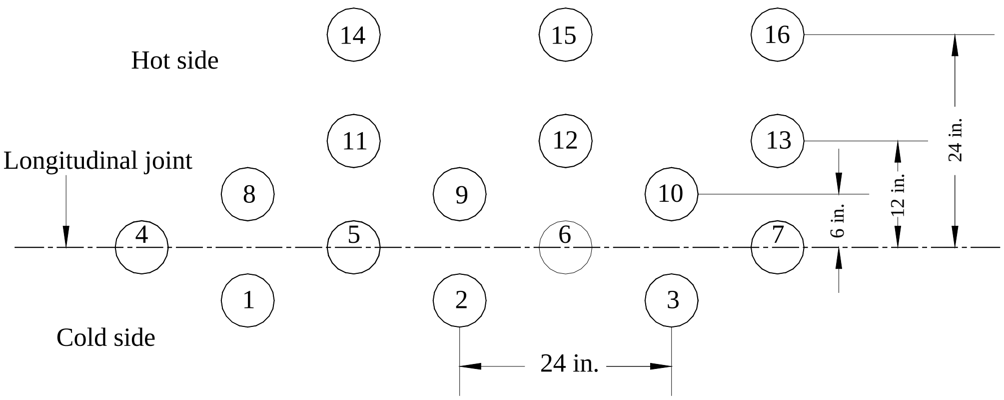


Figure 3-10 Coring Pattern for Project CNG072

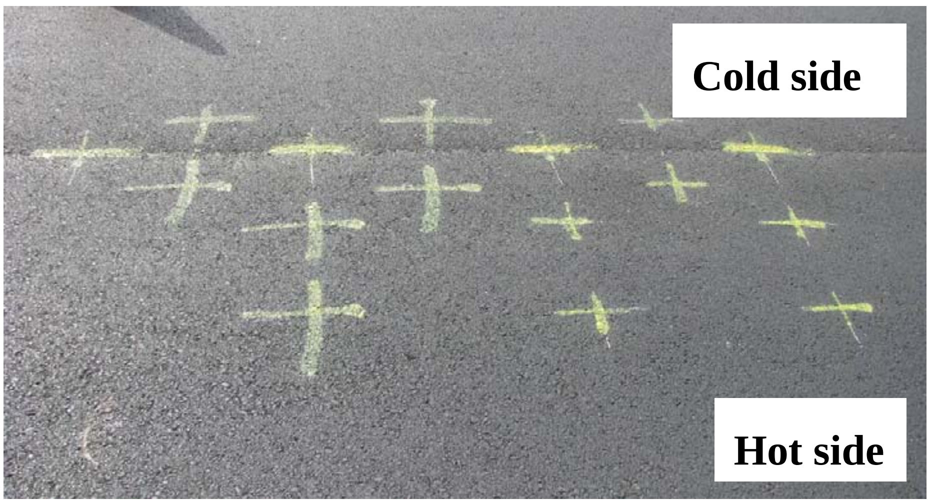


(a) Before Coring


(b) After Coring

Figure 3-11 Core Positions at One Coring Location

Figure 3-12 Field Coring

Figure 3-13 Field Cores Taken at One Location

### 3.1.3 Project CNG155

The Project CNG155 was a pavement resurfacing on State Route (SR) 289 in Sparta, Tennessee (Figure 3-14) with an HMA overlay of approximately 31.8 mm (1.25 in.). Part of the south-bound lane of SR 289 was constructed with different longitudinal joint construction techniques on September 23, 2008 and the north bound lane was completed on the previous day. The test section layout is presented in Table 3-2. Every test section is long enough to examine the effect of joint products on joint construction quality (Kandhal et al. 2002). The same compaction method as usually used in Tennessee was employed for all the test sections to eliminate the effect of different compaction methods on joint construction quality.

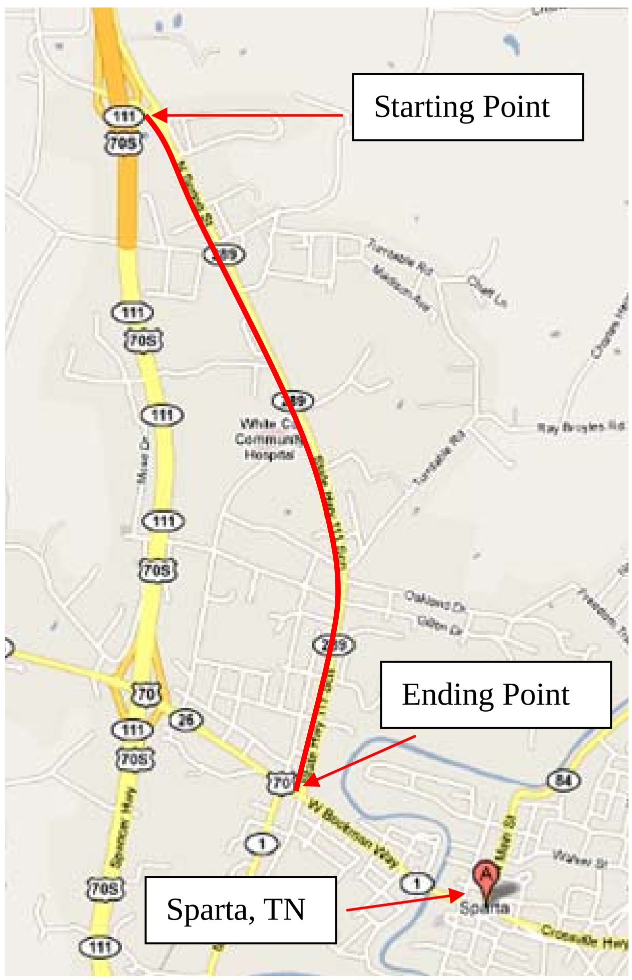


Figure 3-14 Location of Project CNG155

The nominal maximum aggregate size (NMAS) of the HMA mix was 12.5 mm and the mix design is given in Table 3-3.

Seven different construction techniques or products were applied to this project. Based upon their expected mechanisms, these seven techniques could be divided into three main categories: joint adhesives, joint sealers, and infrared heater. The following sections give a brief description of these joint construction products.

Table 3-2 Test Section Layout

| Section Number | Length | Technique or Product | Content of Product and/or Application Method |
|---|---|---|---|
| 1 | 305 m (1000 ft) | Crafco ioint adhesive | Highly polymer (SBS) modified asphalt containing rubber. Applied on the joint surface. Its application rate is 0.25-0.37 kg/m (4-6ft/lb). |
| 2 | 305 m (1000 ft) | Jointbond (joint sealer) | polymerized maltene emulsion and its application rate is approximately 0.36 $L/m^2$ (0.08 $gallon/yd^2$). |
| C1 | 305 m (1000 ft) | Control section | No special treatment |
| 3 | 168 m (550 ft) | Pavon joint adhesive | An emulsion containing SBR polymer and resins. Application rate is approximately 0.17 kg/m (73 gallon/mile) for ½" thick pavements or 0.094 kg/m (40 gallon/mile) for 1" thick pavements. |
| 4 | 293 m (960 ft) | Replay joint sealer | A liquid mixture of agricultural oil (soy bean oil) containing SBS polymer and its application rate is 0.14 $L/m^2$ (0.03 $gallon/yd^2$). |
| 5 | 305 m (1000 ft) | Infrared joint heater | Infrared heating |
| 6 | 305 m (1000 ft) | Polymer emulsion (joint adhesive) | A polymerized emulsion commonly used by TDOT. Its application rate is 0.096-0.11 kg/m (0.07-0.08 $gallon/yd^2$). |
| 7 | 305 m (1000 ft) | Basic emulsion (joint adhesive) | A basic emulsion commonly used by TDOT. Its application rate is approximately 0.124 kg/m (10 gallon/1000 ft). |
| C2 | 473 m (1553 ft) | Control section | No special treatment |

Table 3-3. Mix Proportion for Project CNG155

| Aggregate Composition | |
|---|---|
| Percent Used | Source |
| 50 | #7, Medium Coarse Sandstone, Allons, TN |
| 25 | #10, Soft limestone screening, Sparta, TN |
| 25 | Natural sand, Monterey, TN |
| **Blend Gradation** | |
| Sieve | Percent Passing |
| 16 mm (5/8″) | 100 |
| 12.5 mm (1/2″) | 97 |
| 9.5 mm (3/8″) | 80 |
| 4.75 mm (No.4) | 58 |
| 2.36 mm (No.8) | 41 |
| 0.6 mm (No.30) | 27 |
| 0.3 mm (No.50) | 14 |
| 0.15 mm (No.100) | 6.8 |
| 0.075 mm (No.200) | 5.1 |
| **Mix Design Information** | |
| Design Air Voids (%) | 4 |
| Optimum Asphalt Content (%) | 5.7 |
| AC Grade | PG 64-22 |
| Mixing Temperature (°F) | 290-320 |
| Tensile Strength Ratio (%) | 83.5 |
| Marshall Stability (lb) | 4017 |
| Marshall Flow (0.01 in.) | 12.5 |

#### 3.1.3.1 Joint Adhesives

Four joint adhesives were applied to the joint surface before placement and compaction of asphalt mixture, with the aim to improve the bonding between cold and hot lanes and to help prevent rainfall from penetrating into joint (Figure 3-15). They included two commercially available joint adhesives (Crafco and Pavon joint adhesives), and two emulsions commonly used by TDOT as tack coat. Crafco joint adhesive is a hot-applied high-polymer (SBS) asphalt containing rubber typically applied at 0.25-0.37 kg/m (4-6 ft/lb), see Figure 3-15(a). Figure 3-15(b) shows that the temperature of Crafco joint adhesive was tested to be around 182°C (360°F) immediately after application. Pavon joint adhesive is a highly polymerized emulsion containing SBR polymer and resins, see Figure 3-15(c). Its application rate is approximately 0.17 kg/m (73 gallon/mile) for ½" thick pavements and 0.094 kg/m (40 gallon/mile) for 1" thick pavements. The two emulsions used by TDOT as joint adhesive in this study were a polymer emulsion and a basic emulsion. The polymer emulsion was spray applied at a rate of 0.096-0.11 kg/m (0.07-0.08 gallon/yd$^2$) along the longitudinal joint approximately 30.5 cm (12 in.) wide before placement of the adjacent lane, see Figure 3-15(d). The basic emulsion was manually applied along the longitudinal joint and its application rate was 0.124 kg/m (10 gallons/1000 ft), see Figure 3-15(e).

(a) Crafco Joint Adhesive

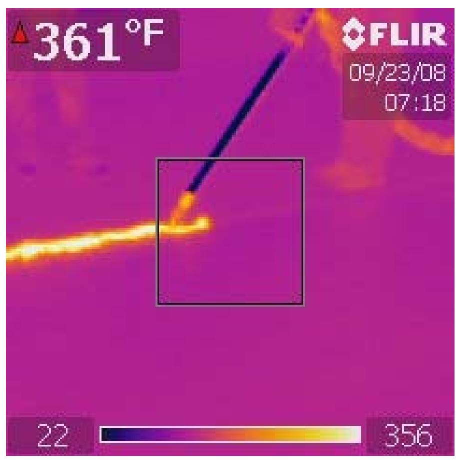


(b) Infrared Photo from Crafco Joint Adhesive

(c) Pavon Joint Adhesive

(d) Polymer Emulsion

(e) Basic Emulsion

Figure 3-15 Application of Joint Adhesives

### 3.1.3.2 Joint Sealers

Two joint sealers were employed (Jointbond and Replay joint sealers) to prevent rainfall from penetrating into asphalt pavement. Joint sealers were spray applied to the joint area after pavement compaction. Jointbond is a polymerized maltene emulsion and its application rate is usually 0.36 $L/m^2$ (0.08 $gallon/yd^2$), see Figure 3-16(a). Replay joint sealer is a liquid mixture of agricultural oil (soy bean oil) containing SBS polymer and its application rate is 0.14 $L/m^2$ (0.03 $gallon/yd^2$), see Figure 3-16(b).

(a) Jointbond

(b) Replay Joint Sealer

Figure 3-16 Application of Joint Sealers

#### 3.1.3.3 Infrared Joint Heater

The infrared joint heater was used to preheat the cold edge of the previously compacted lane with infrared heat converted from a propane fired heater before placement of asphalt mixture. The purpose of the preheating is to improve the adhesion between cold and hot lanes and make pavement compaction easier. The joint heating system consists of several heaters towed by a tractor [Figure 3-17(a)] and one heater attached to the paver [Figure 3-17(b)]. Immediately after heating, the joint temperature could reach up to 250°F. The joint temperature dropped down to approximately 230°F before mixture placement [Figure 3-17(c)].

(a) Towed Infrared Heater

(b) Heater Attached to the Paver


(c) Infrared Photo of Joint Heater

Figure 3-17 Infrared Joint Heater

#### 3.1.3.4 Field Coring

Two coring patterns were used to take cores from the longitudinal joint and its neighboring area to investigate the joint quality. For the test sections of the infrared joint heater and the second control section, the coring pattern as shown in Figure 3-18 was used to take 11 field cores. For the rest of the test sections, only seven cores (No. 1 to 7) were taken to reduce the damage caused by the coring to the pavement. The field coring began the next day after construction and finished within three days.

The field cores were 150 mm (6 in.) in diameter. Some field cores contained more than the surface overlay layer and they were cut into 31.8 mm (1.25 in.) thickness, the same thickness as that of the overlay. During the cutting, caution was taken to make sure that the cutting surface was parallel to the top surface of the field cores. The 31.8 mm thick field cores were then used as test specimen for the laboratory tests.

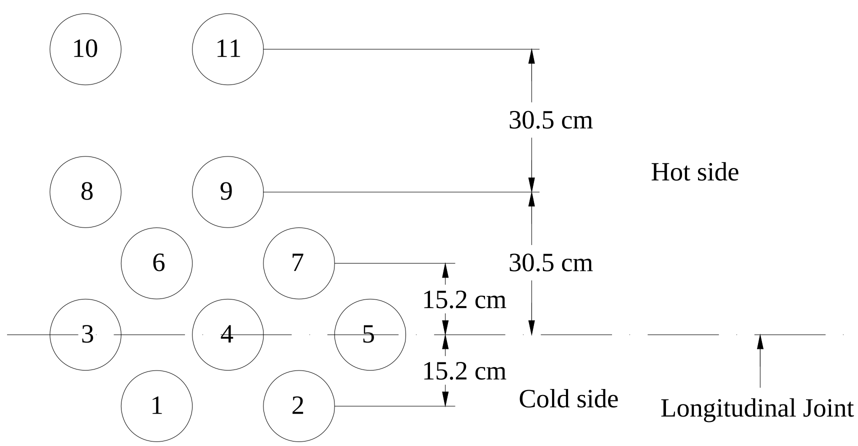


Figure 3-18 Coring Pattern (Cores No. 8 through 11 were taken only for the infrared joint heater and the second control sections)

## 3.2 Laboratory Tests

Several laboratory tests were conducted to determine the effects of these joint techniques on joint quality. Laboratory tests were performed on the 150-mm diameter and 31.8 cm thick field cores. Laboratory tests included determination of bulk specific gravity of cores according to ASTM D2726, water permeability test, water absorption test, indirect tensile (IDT) strength test, and X-ray Computed Tomography (CT) test. Air void content was calculated using bulk specific gravity of field cores and the maximum specific gravity obtained from the asphalt mixture test conducted by the TDOT quality assurance (QA) personnel on the jobsite.

### 3.2.1 Permeability Test

A falling head permeameter was used to determine the water permeability of the field cores (Figure 3-19). While water flows in the vertical direction through the test specimen, the time interval for the water head to drop from the initial reading to the final reading is recorded. Based on Darcy's law, the coefficient of permeability is expressed using the following equation:

$$k = \frac{aL}{At} \ln\left(\frac{h_1}{h_2}\right) \times t_c \tag{3-1}$$

where $k$ = coefficient of permeability; $a$ = inside cross-sectional area of standpipe; $L$ = average thickness of the core; $A$ = average cross-sectional area of the core; $t$ = elapsed time between $h_1$ and $h_2$; $h_1$ = initial head across the core; $h_2$ = final head across the core; and $t_c$ = temperature correction for viscosity of water.

Figure 3-19 Water Permeameter

### 3.2.2 Water Absorption Test

To identify the mechanism of joint sealers for protecting longitudinal joints, a water absorption test (Figure 3-20) was developed and conducted only on the joint cores to investigate whether joint sealers could prevent water from penetrating into the joint. Field cores were submerged in the water bath at 25°C for 40 min. Then they were surface dried with a damp cloth and immediately covered with a 150 mm diameter paper cloth. The paper cloth was gently pressed against the top surface to make sure that they were in close contact with each other. The water absorption rate is defined as:

$$\text{Absorption Rate} = \frac{W_2 - W_1}{W_1} \times 100 \quad (3\text{-}2)$$

where Absorption Rate = water absorption rate, %; $W_1$ = initial dry weight of paper cloth; and $W_2$ = final weight of paper cloth.

(a) Field Cores Covered with Paper Cloth

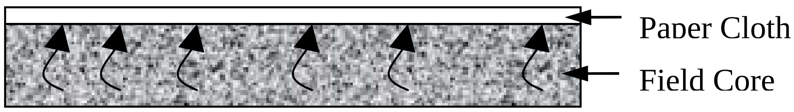


(b) Scheme of Water Absorption

Figure 3-20 Water Absorption Test

### 3.2.3 IDT Strength Test

The IDT strength test (Figure 3-21) was used to determine tensile strength of field cores, which could be an indicator of adhesion between cold and hot lanes for joint cores. In this test, field cores were monotonically loaded to failure along the vertical diametric axis at a constant rate of 76.2 mm/min. For joint cores, caution was taken to make sure that the specimens were loaded along the direction of the longitudinal joint so that failure could occur along the joint and the indirect tensile strength along the joint was measured. The indirect tensile strength can be calculated as follows:

$$S_t = \frac{2P}{\pi D t} \quad (3\text{-}3)$$

where $S_t$ = indirect tensile strength; $P$ = failure load; $D$ = diameter of specimen; and $t$ = thickness of specimen.

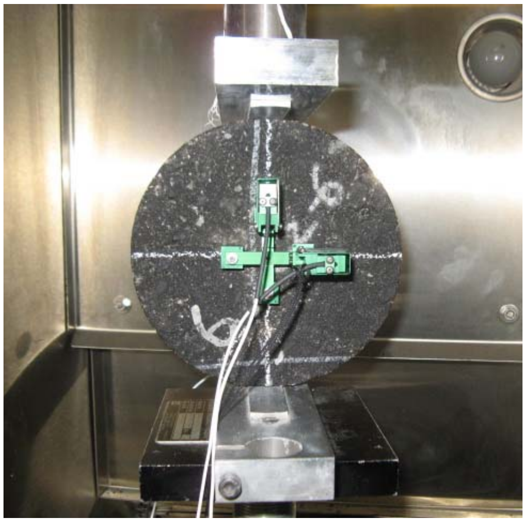

Figure 3-21 IDT Test Setup

### 3.2.4 X-ray CT Test

Some field cores were selected and scanned with the X-ray CT machine (Figure 3-22). X-ray particles emitted from the X-ray source penetrate through the core and are detected by an X-ray detector. Due to the difference in attenuation of X-ray particles penetrating through the individual components of asphalt mixtures, 2-D X-ray images are obtained from the detected X-ray intensity. In the study, 2-D images were acquired every 1 mm along the depth of field cores. The air voids distribution along the vertical direction was then obtained through image processing technique.

Figure 3-22 X-ray CT Machine

# CHAPTER 4 LABORATIORY TEST RESULTS AND DISCUSSION

## 4.1 Project CNF923

The air voids, water permeability, and indirect tensile (IDT) strength tests were conducted on the field cores taken from the longitudinal joint area of the Project CNF923. Since the field cores were taken twice from the Project CNF923, the test results for the cores taken on the first time are presented in Table 4-1 and Figures 4-1, 4-2, and 4-3. The relationship between the joint construction quality and the distance from the longitudinal joint is shown in Figures 4-4, 4-5, and 4-6.

Table 4-1 Test Results of Cored Samples

| Core No. | Air voids (%) | Permeability Coef. k ($\times 10^{-5}$ cm/s) | IDT Strength (psi) |
|---|---|---|---|
| 3 | 8.2 | 67.1 | 209.2 |
| 4 | 7.8 | 50.1 | 191.6 |
| 5 | 7.5 | 29.5 | 174.2 |
| 8 | 8.2 | 87.9 | 181.6 |
| 9 | 8.7 | 152.2 | 175.8 |
| 10 | 9.8 | 198.4 | 158.3 |
| 11 | 10.3 | 351.7 | 156.7 |

Note: Cores No. 3 to 5 were taken on the longitudinal joint. Cores No. 8 and 9 were taken on the hot side 6 inches away from the joint. Cores No. 10 and 11 were taken 12 inches away from the joint on the hot side.

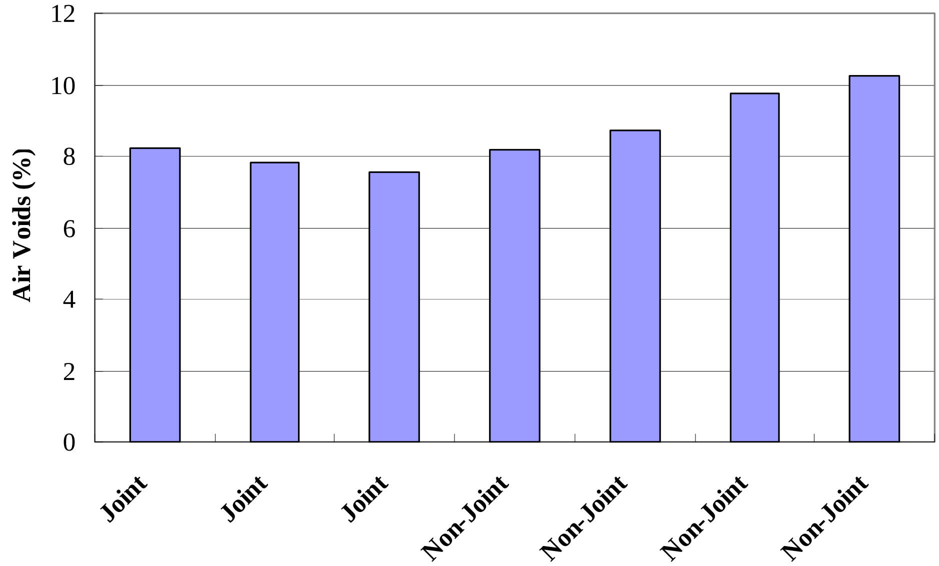


Figure 4-1 Air Voids Results

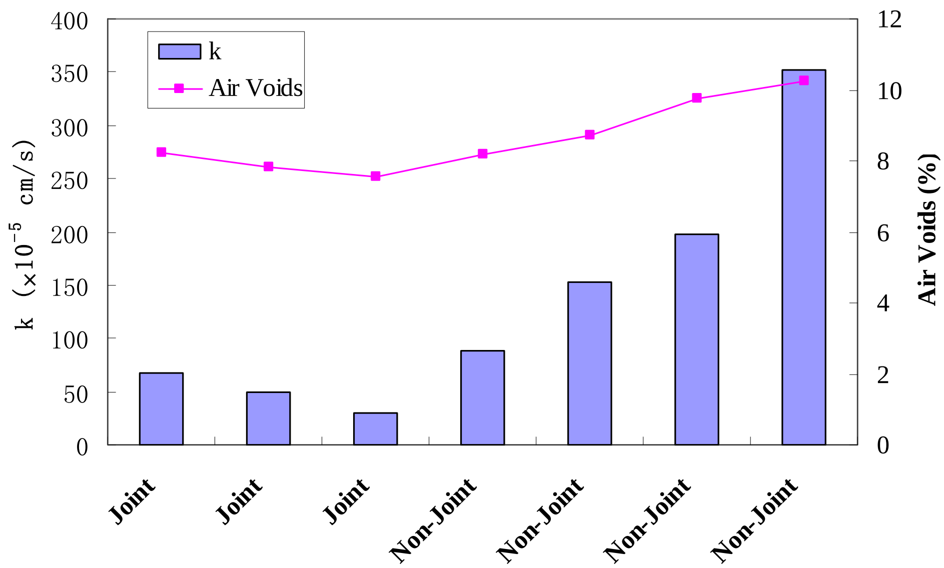


Figure 4-2 Water Permeability Results

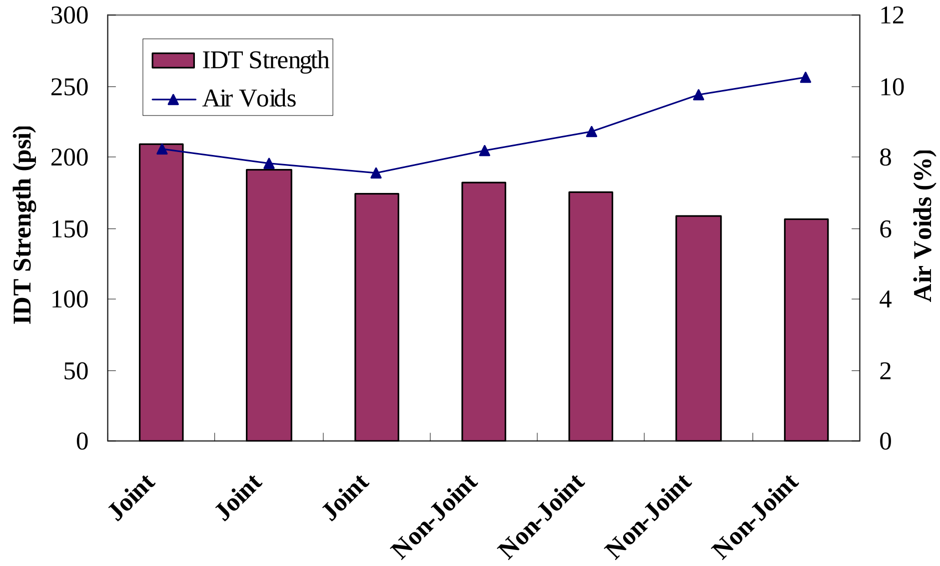


Figure 4-3 IDT Strength

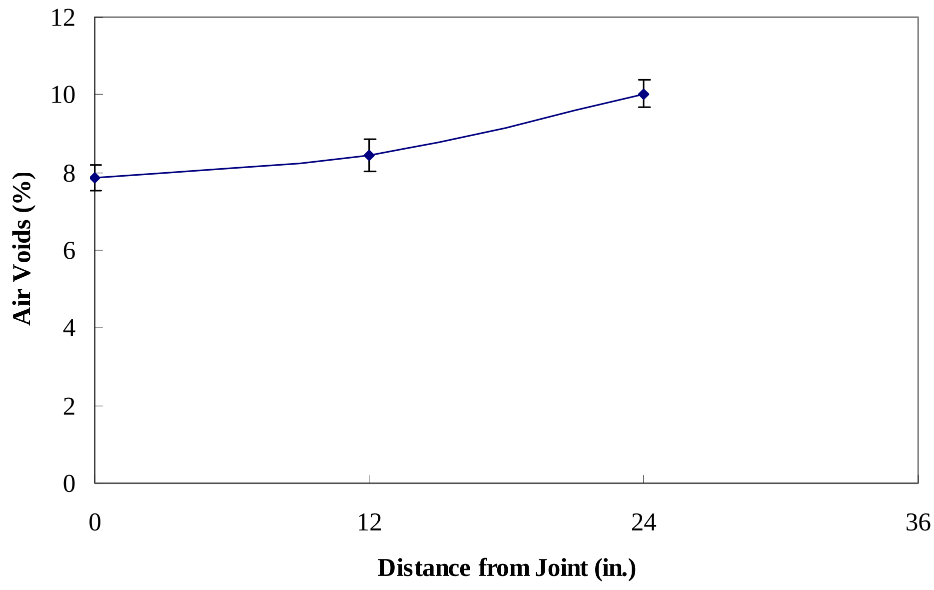


Figure 4-4 Change of Air Voids with Location

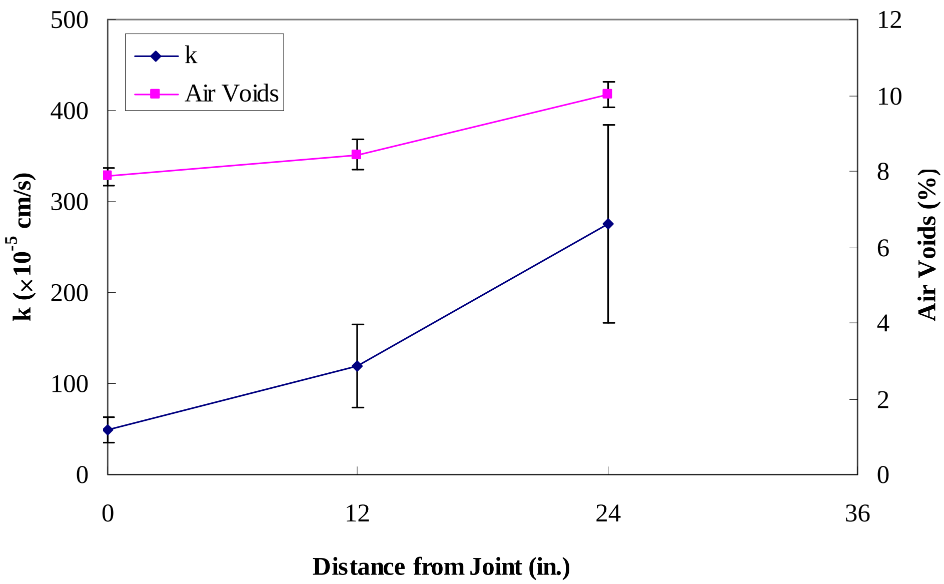


Figure 4-5 Change of Water Permeability with Location

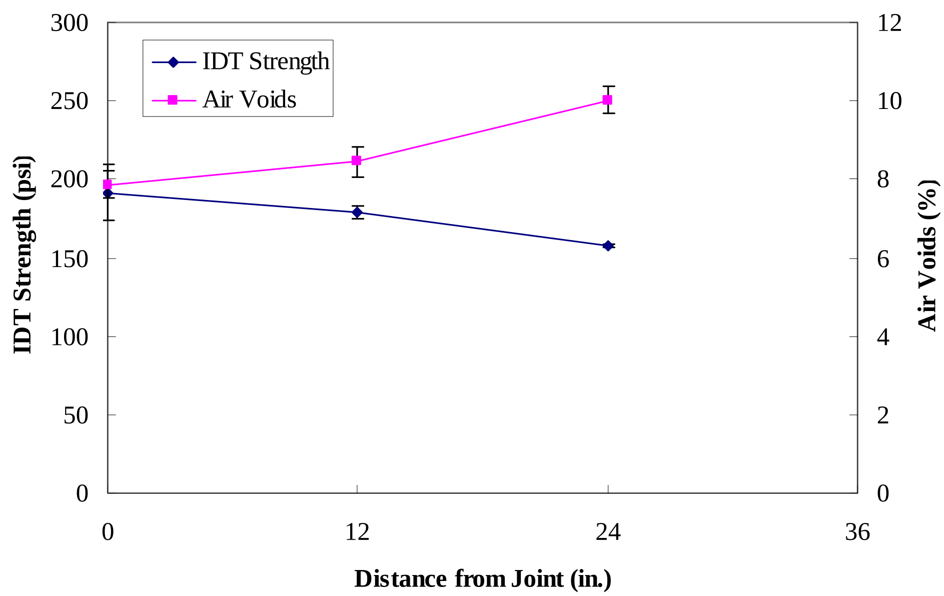


Figure 4-6 Change of IDT Strength with Location

From Table 4-1 and Figures 4-1 to 4-3, it can be seen that the cores taken from the longitudinal joint exhibited lowest air void content, lowest water permeability, and highest IDT strength, which indicates that good joint construction quality could be achieved through the adoption of infrared heating technique. Figures 4-4 to 4-6 further clearly show that the closer the distance from the longitudinal joint, the better the joint construction quality, which can also be attributed to the joint heating technique. The results from the three laboratory tests were consistent with each other, i.e., the lower the air void content, the lower the water permeability, the higher the IDT strength, and the better the joint construction quality.

Figures 4-7, 4-8, and 4-9 graphically present the test results for the cores taken on the second time. The results from the three tests were also found to be consistent with each other, which means that generally high air void content leaded to high permeability and low IDT strength. However, unlike the results for the first coring, the results for the second coring show that the best construction quality was achieved at an area near the longitudinal joint on the hot side, not on the longitudinal joint. Although the joint heating technique was applied for this project, the longitudinal joint and the cold side edge area still exhibited higher air void content, higher permeability, and lower IDT strength when compared to the hot side construction quality. The test results from the cores at three different coring locations generally follow the similar trend.

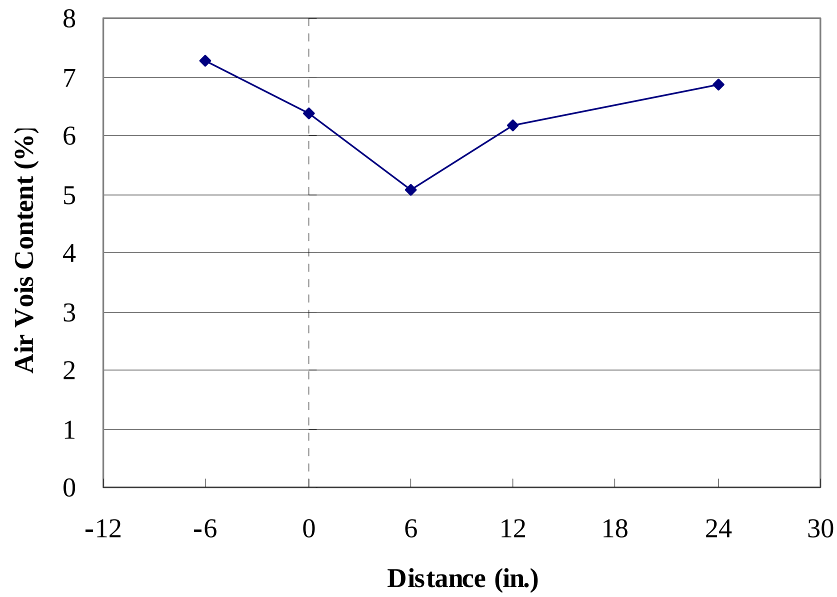


(a) Spot A

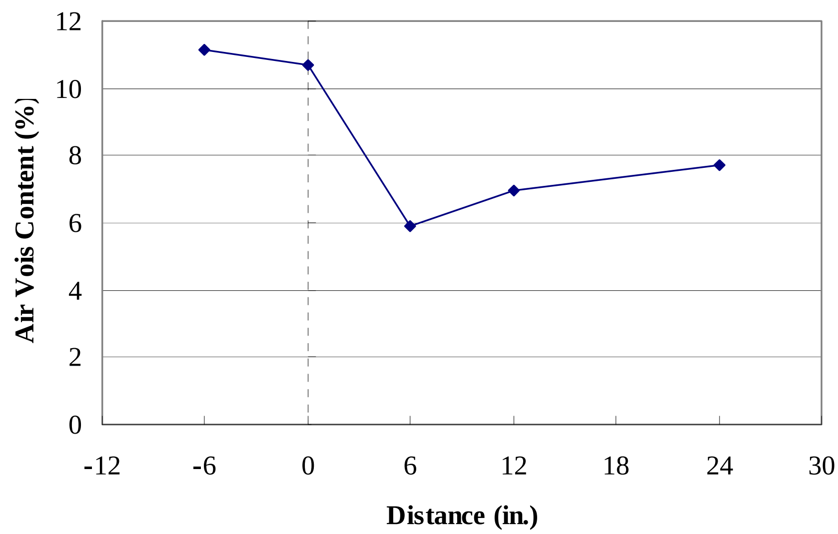


(b) Spot B

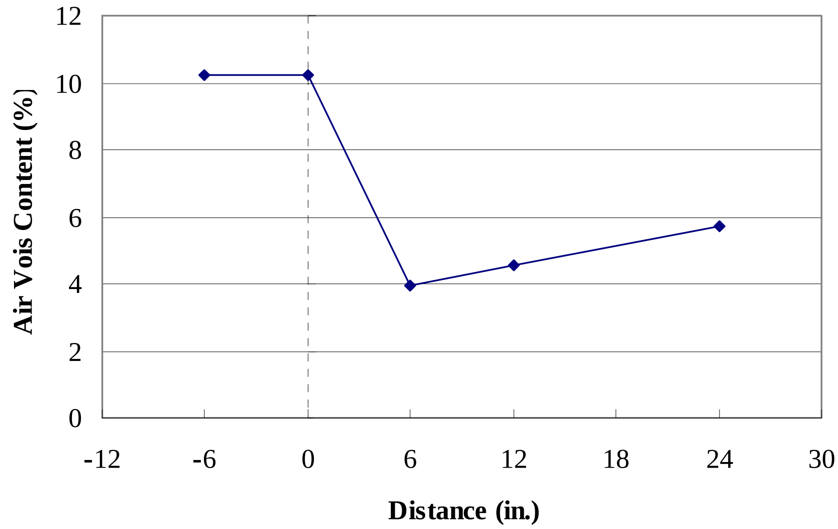


(c) Spot C

Figure 4-7 Air void content Results

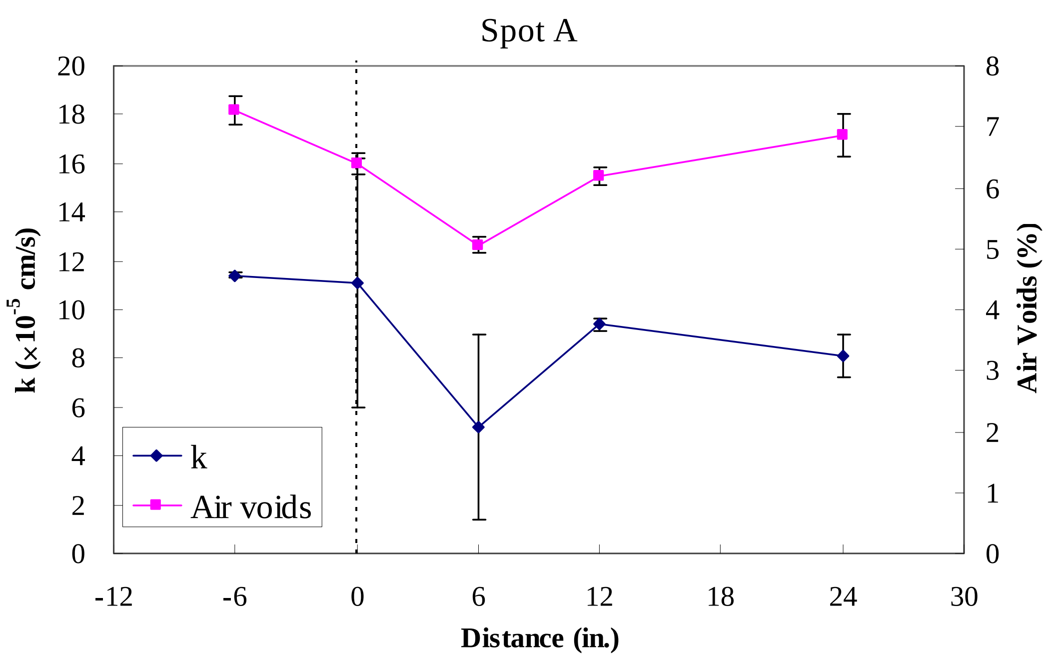


(a) Spot A

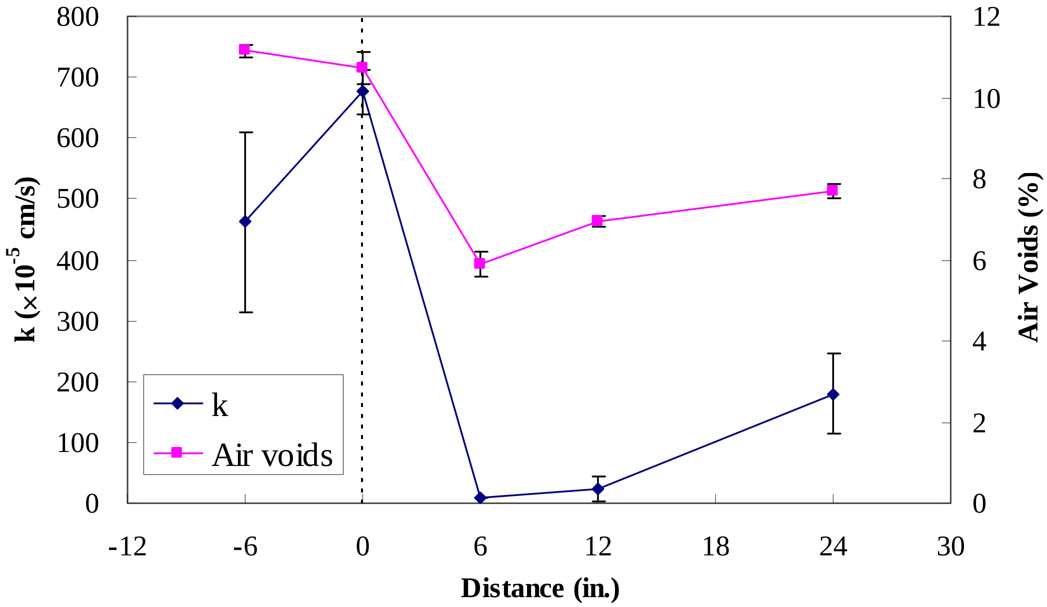


(b) Spot B

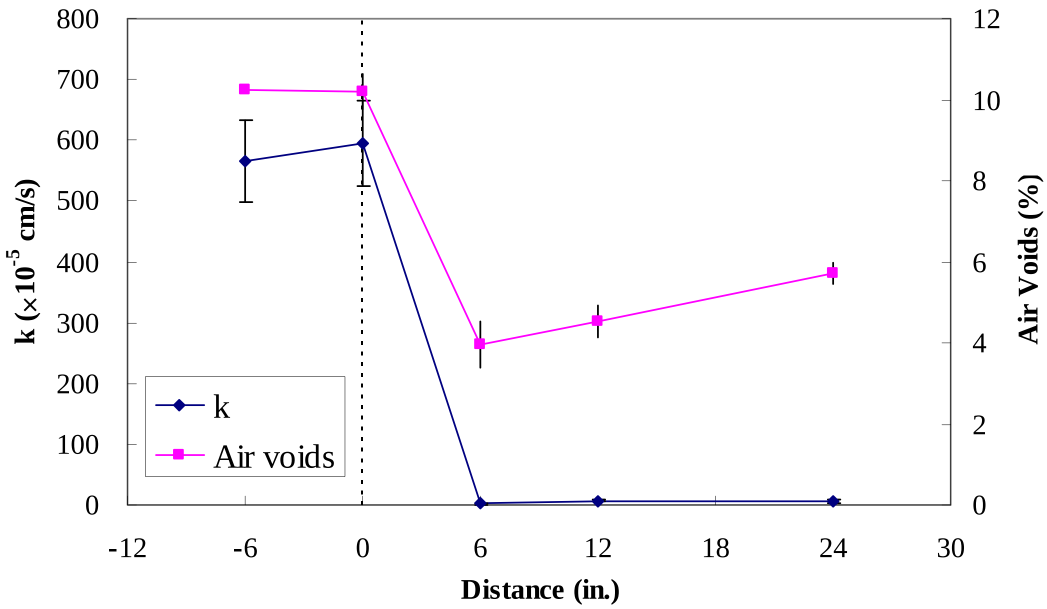


(c) Spot C

Figure 4-8 Permeability Results

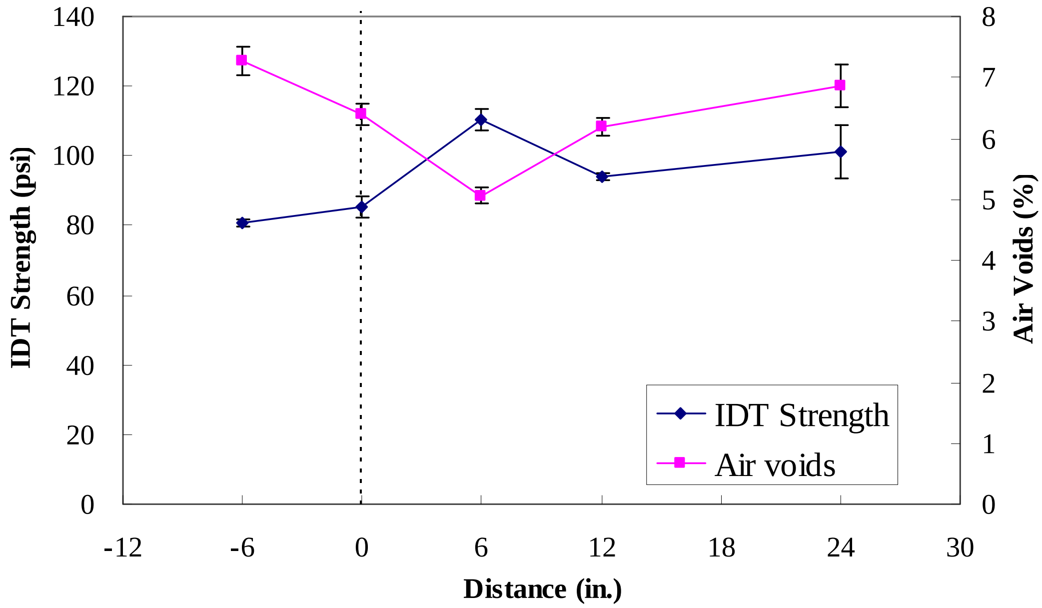


(a) Spot A

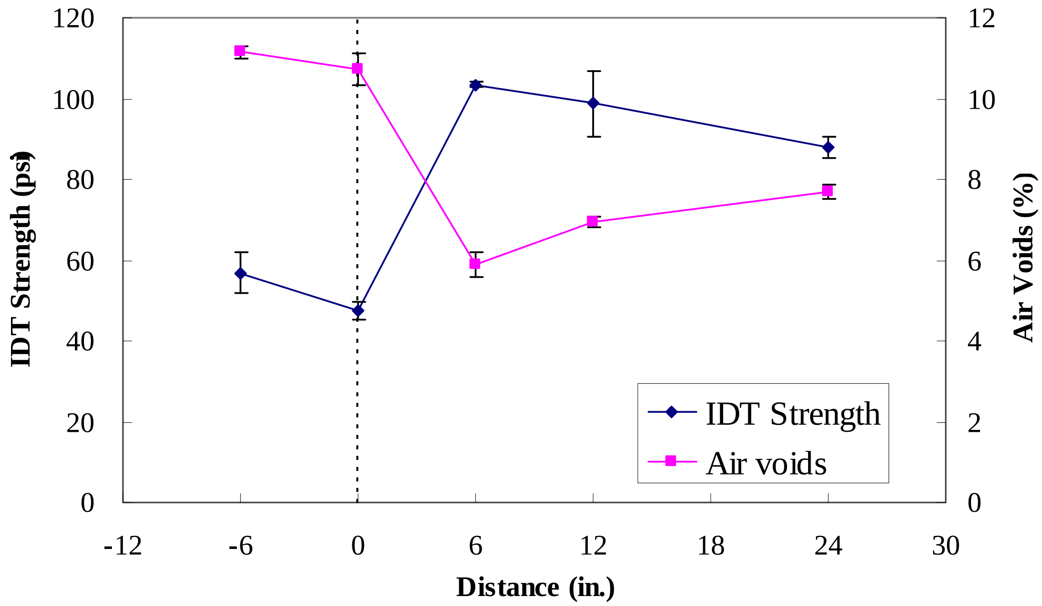


(b) Spot B

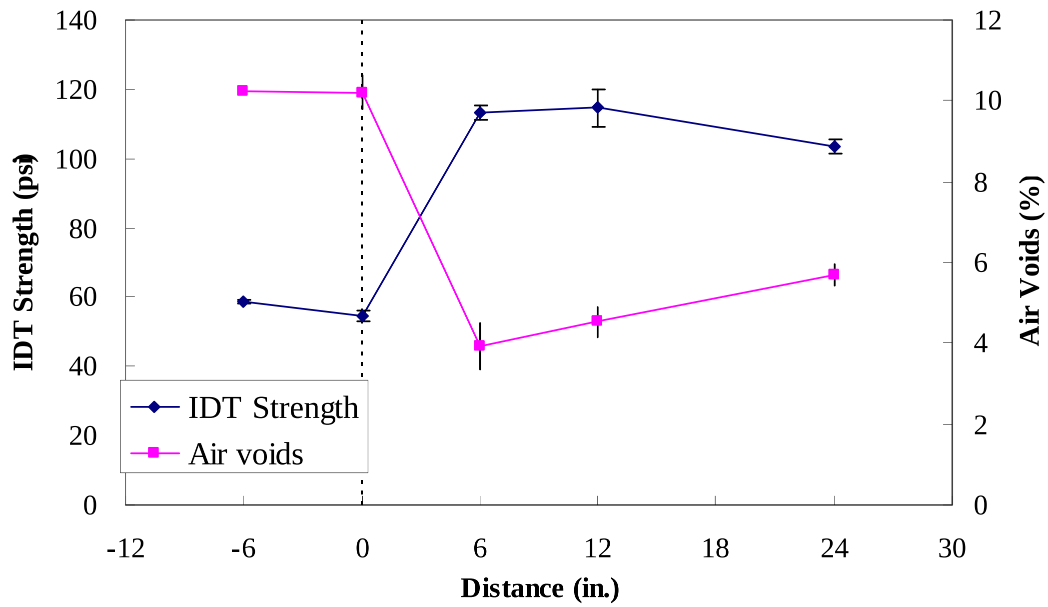


**(c) Spot C**

Figure 4-9 IDT Strength Results

## 4.2 Project CNG072

The air void content, permeability, and IDT strength tests were conducted on the field cores taken from the Project CNG072. Figures 4-10, 4-11, and 4-12 graphically present the test results. The results from the tests were consistent with each other, i.e., the higher the air void content, the higher the permeability, and the lower the IDT strength. It can be seen that without any special joint construction treatment and just using the conventional construction method as usually used in the state of Tennessee, the longitudinal joint exhibited much higher air void content and permeability and much lower IDT strength than its neighboring area on both cold and hot sides. This indicates that longitudinal joint construction quality may not be guaranteed with the conventional construction practice. To improve joint construction quality, special joint construction methods or compaction methods will be needed.

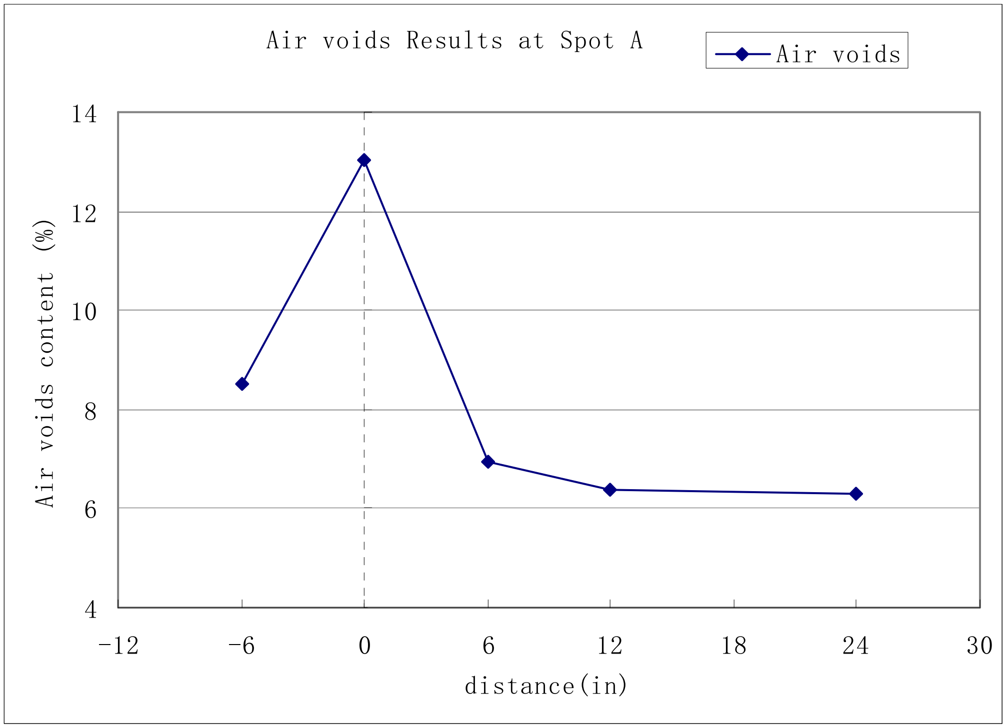


(a) Spot A

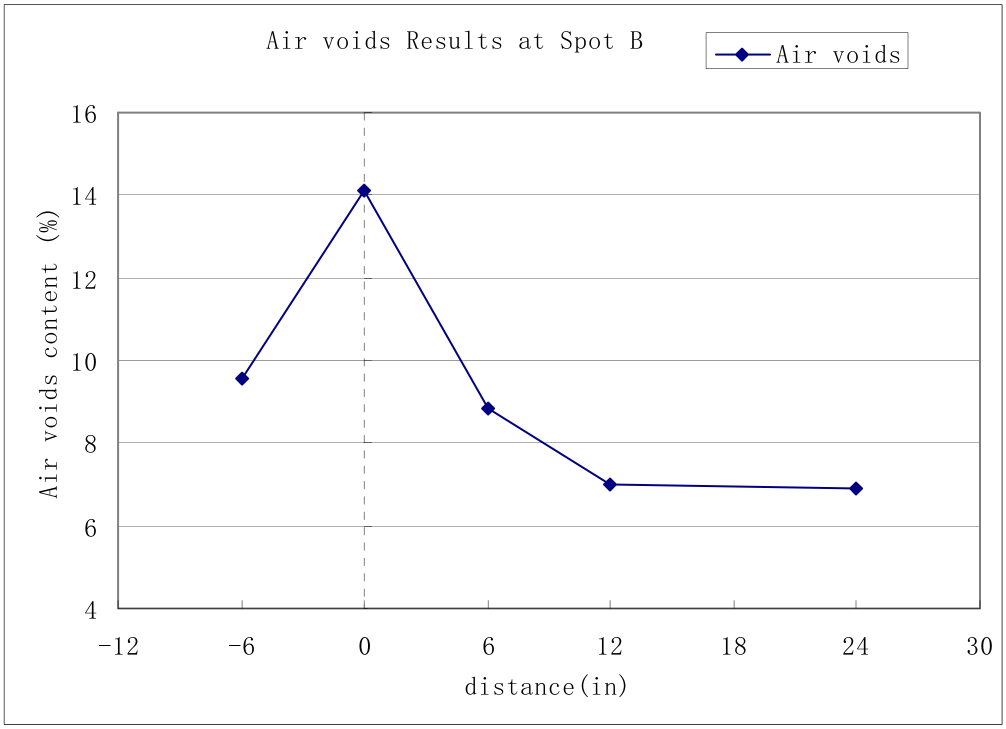


(b) Spot B

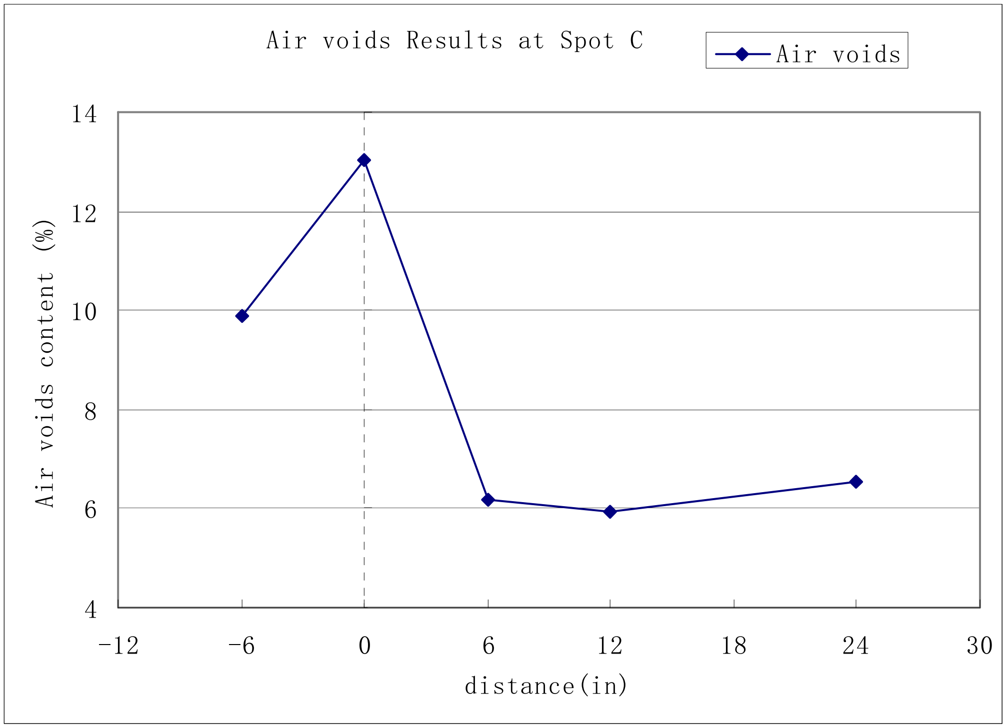


(c) Spot C

Figure 4-10 Air Voids Results

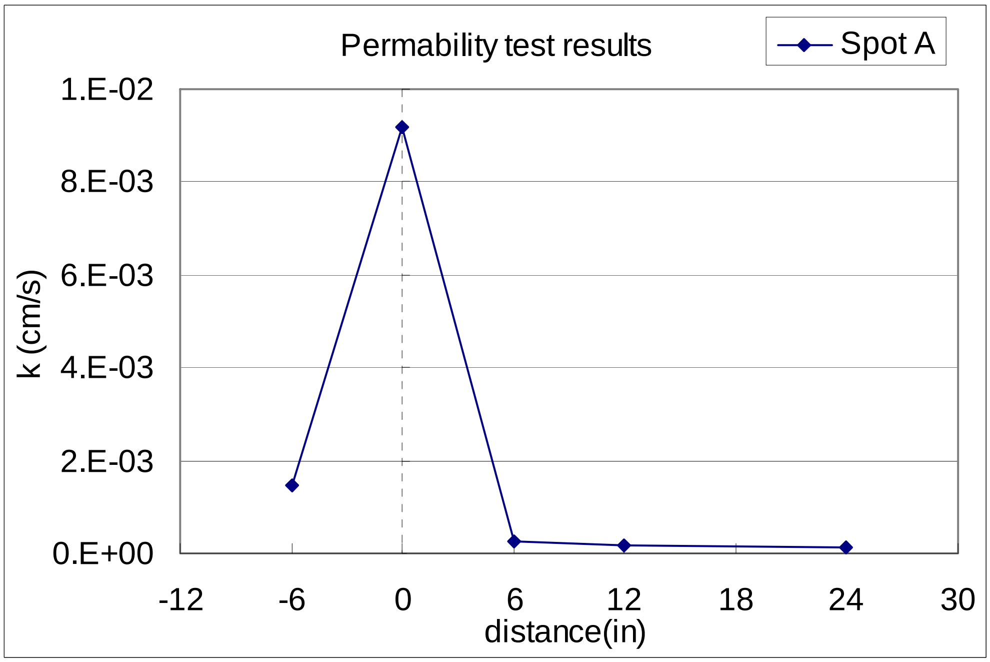


(a) Spot A

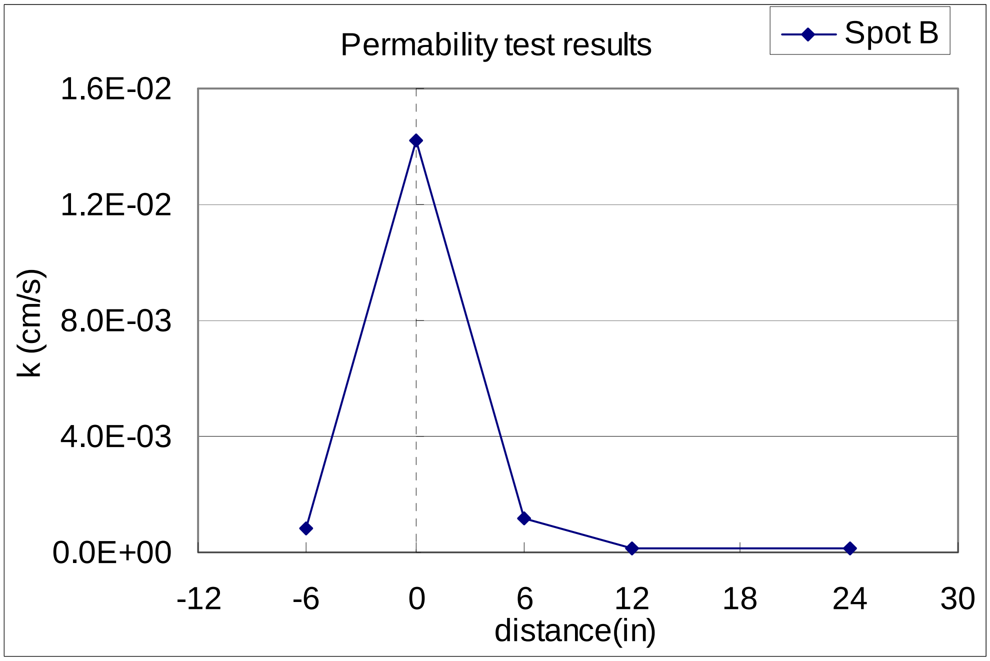


(b) Spot B

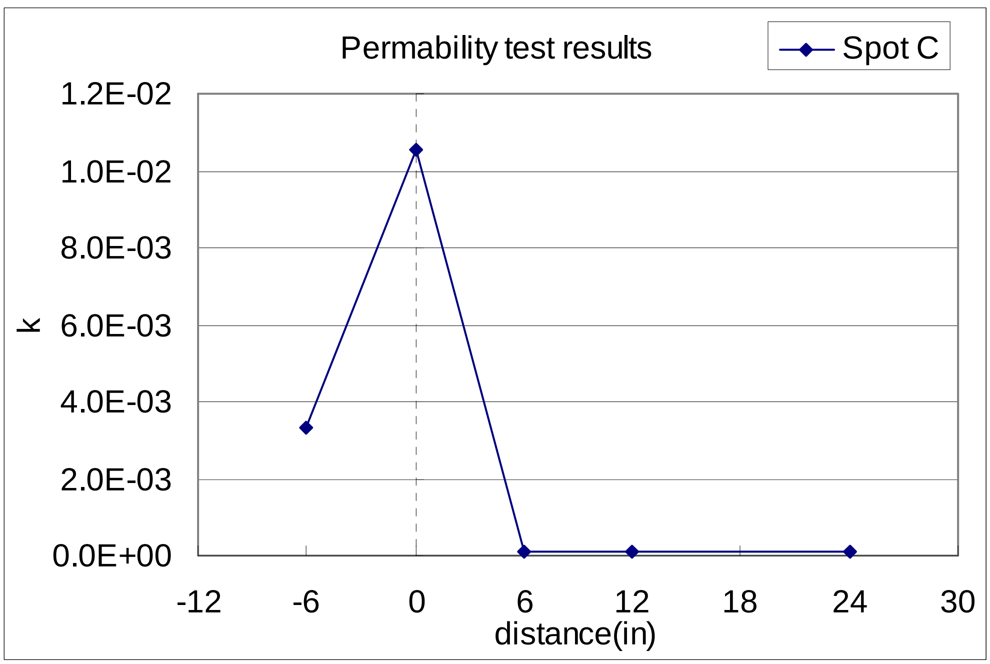


(c) Spot C

Figure 4-11 Permeability Results

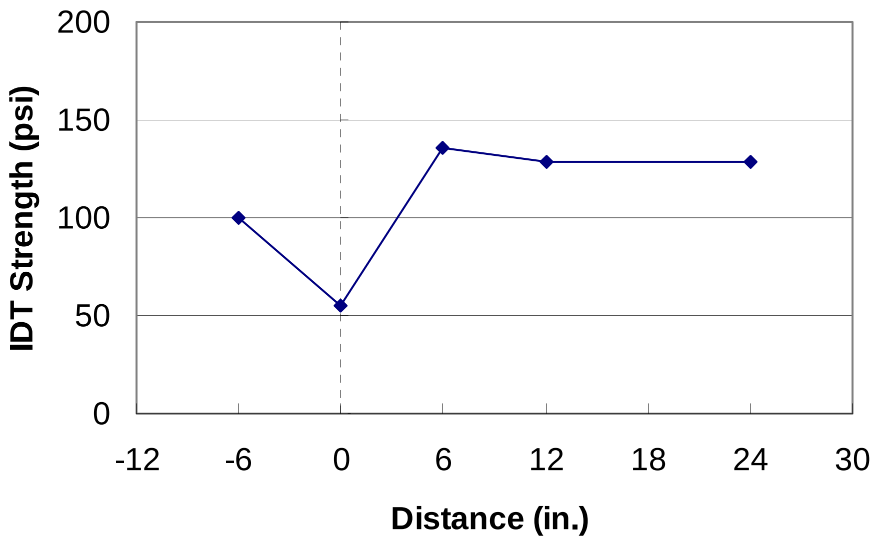


(a) Spot A

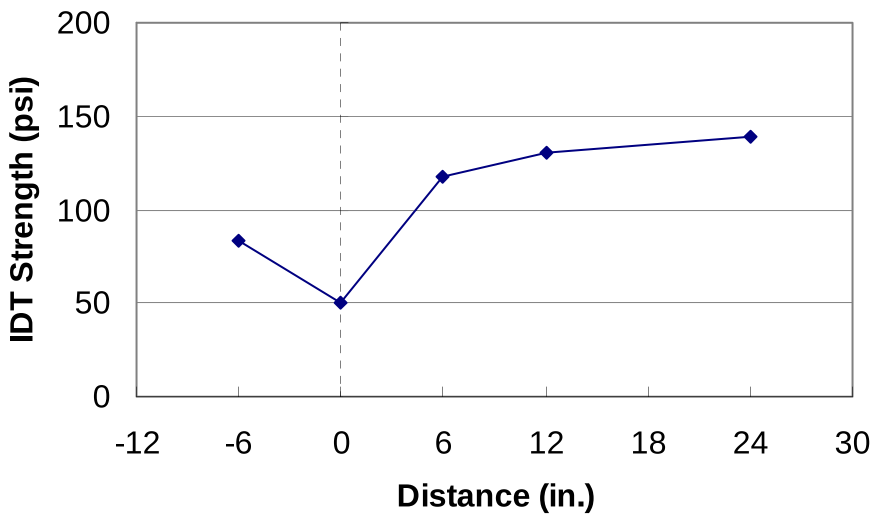


(b) Spot B

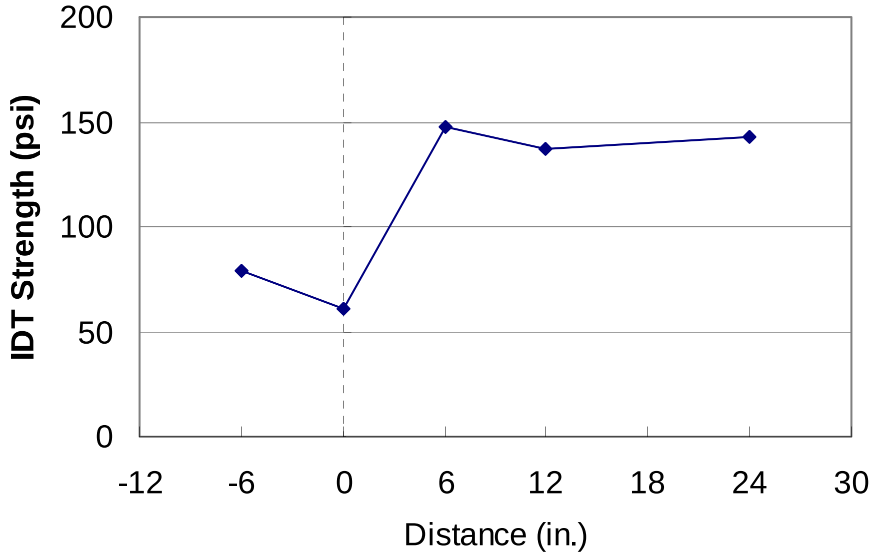


(c) Spot C

Figure 4-12 IDT Strength Results

## 4.3 Project CNG155

### 4.3.1 Air Void Content

The air voids results of the field cores for the Project CNG155 are presented in Figure 4-13. It can be seen from Figure 4-13(a) that without any special joint construction technique, longitudinal joints had the highest air void content followed by the mat on the cold side. The mat on the hot side had the lowest air void content. The high air void content of the cold lane could be attributed to the unconfined state under which the first lane was paved. The existence of the first (cold) lane provided the confinement needed for a good compaction for the second (hot) lane, which resulted in a much lower air void content.

Figures 4-13(b) and (c) show that the air voids distribution across the longitudinal joint for joint adhesives and sealers was similar to that of the control section, which indicates that joint adhesives and sealers did not assist in reducing air void content in the longitudinal joint area. This is consistent with the expected mechanisms for joint adhesive and sealer. The purpose of joint adhesive was to improve the adhesion between cold and hot lanes and the purpose of joint sealer was to seal pavement surface to protect it from water penetrating into it. They were not used to improve the longitudinal joint density.

Unlike joint adhesive and sealer, infrared heater was employed to heat the joint area, to make compaction easier, and thus to compact the joint denser. The effect of infrared heating is clearly shown in Figure 4-13(d). Compared to the test sections of control, joint adhesive, and joint sealer, the air void content of the infrared heat test section was greatly reduced through infrared heating and the longitudinal joint was the densest among all the test sections in this field project. In addition, the construction improvement was not limited to the narrow joint. Even the mat density of the cold side was also improved. As shown in Figure 3-17, a fairly wide area along the joint could be heated and affected by the infrared heater and the construction quality could be improved through the infrared heating.

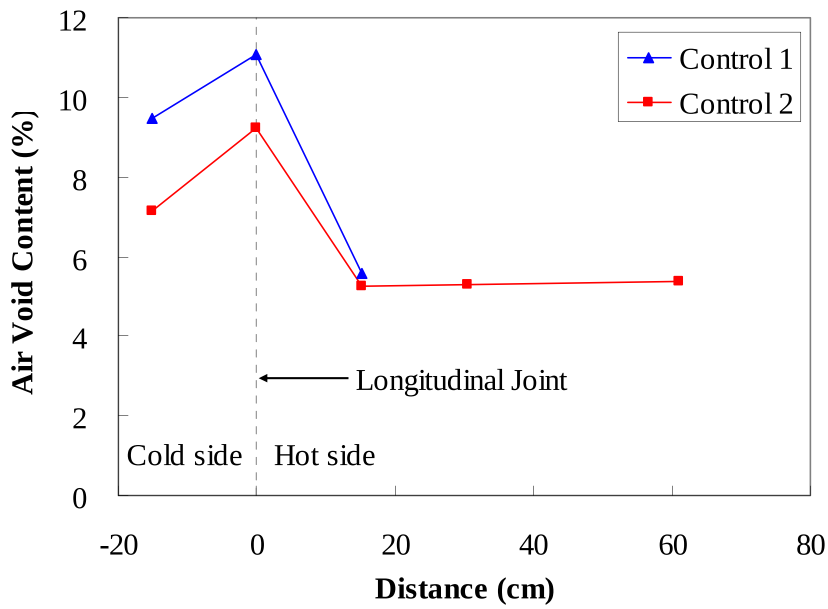


(a) Control

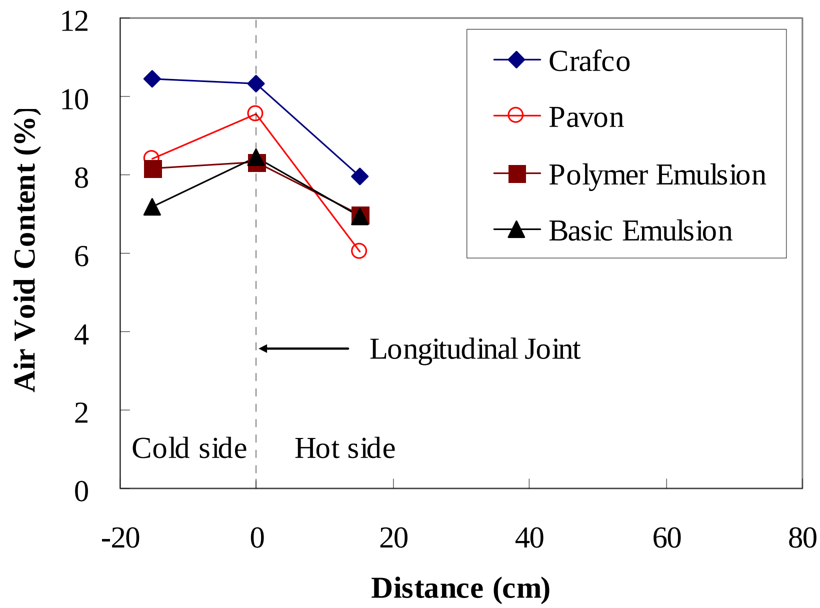


(b) Joint Adhesives

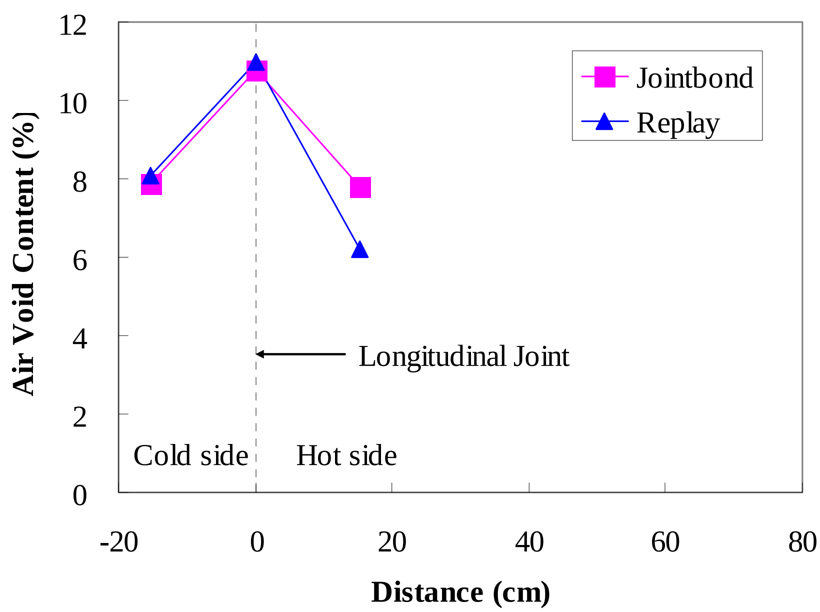


(c) Joint Sealers

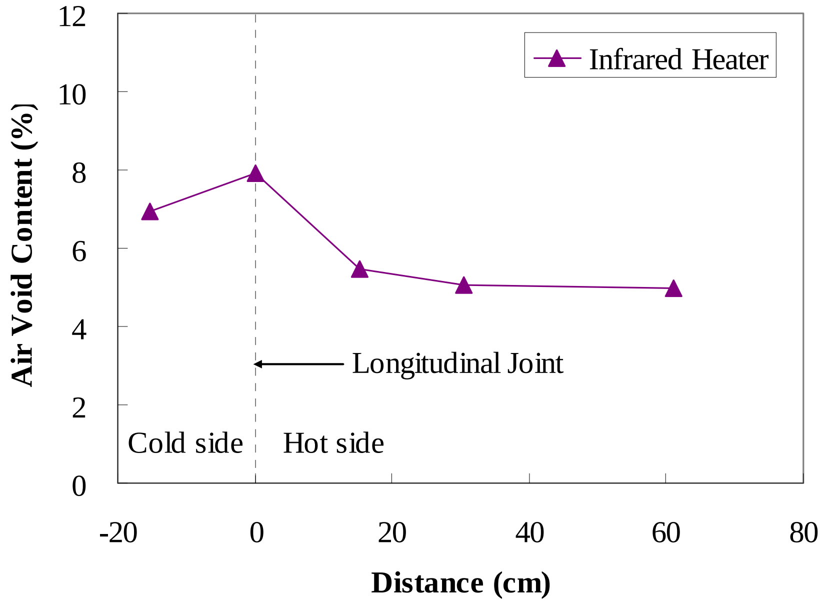


(d) Infrared Heater

Figure 4-13 Air Void Results for Project CNG155

### 4.3.2 Permeability

The coefficients of permeability of the field cores from the Project CNG155 are shown in Figure 4-14. It is observed that the distribution of permeability across the longitudinal joint is similar to that of air void content, i.e., the joint exhibited the highest permeability, followed by the mat on the cold side. The mat on the hot side exhibited the lowest permeability. The permeability results are consistent with those of the air void content because air void is generally directly related with permeability. A high air void content usually leads to a high permeability.

However, it appears that there was no substantial improvement in joint construction quality in terms of permeability for the test sections constructed with the joint sealers (Jointbond and Repaly). The two joint sealer sections exhibited permeability results similar to those of other sections without joint sealer. The reason may lie in the fact that the sealant membrane was not so strong as to withstand the relatively high water head in the falling head permeability test used in this study. However, the sealant membrane may be still effective in preventing water from penetrating into pavement during a regular rainfall, which was confirmed by the results from the water absorption test that will be discussed later.

Figure 4-14(d) shows that the infrared heater was very effective in reducing the permeability coefficient along the longitudinal joint and in its neighboring area. Compared to other test sections, the section of infrared heater exhibited much lower permeability coefficient around the joint area. Since water infiltrating into longitudinal joint plays a significant role in cracking or raveling failure of longitudinal joint, the lower permeability coefficient achieved through infrared heater would help longitudinal joint perform better and last longer.

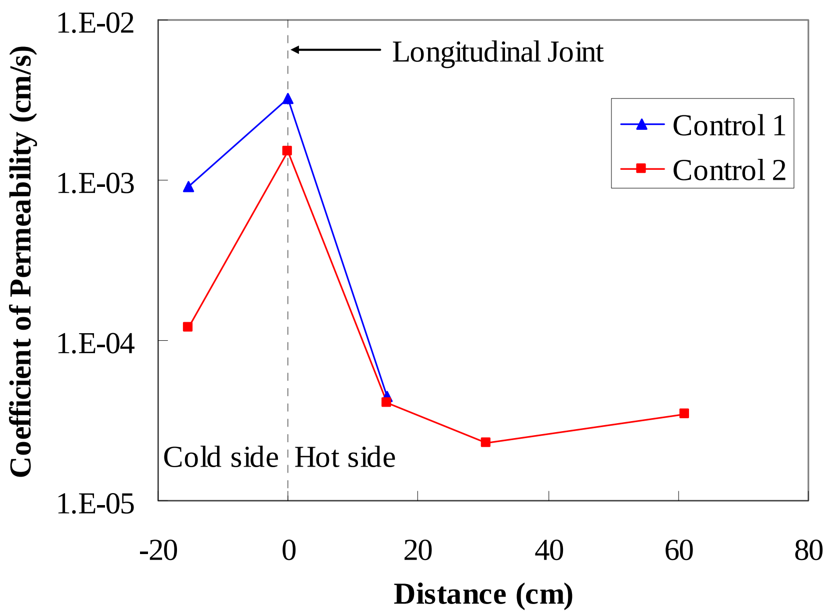


(a) Control

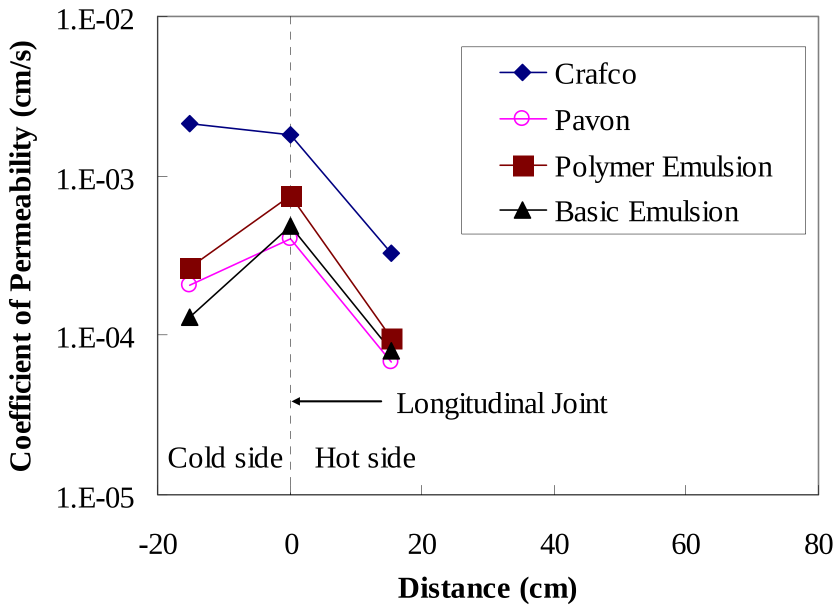


(b) Joint Adhesives

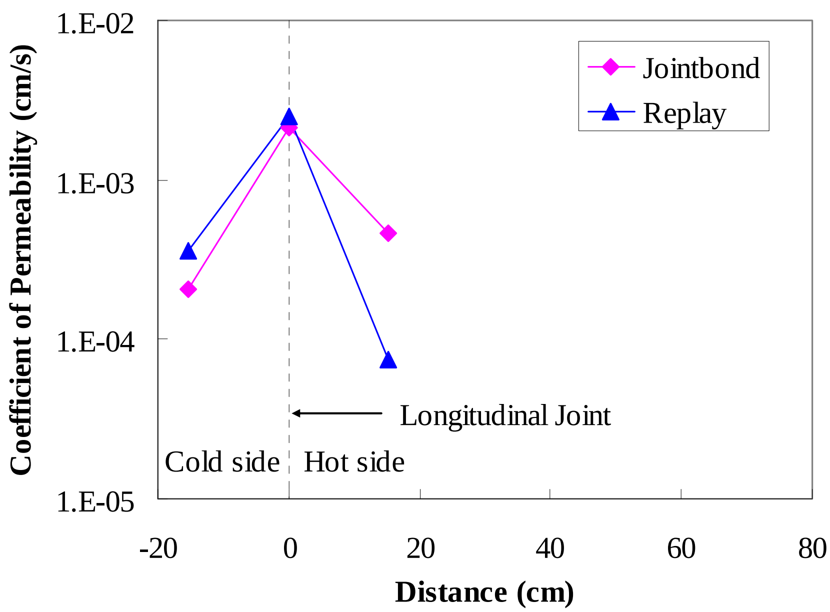


(c) Joint Sealers

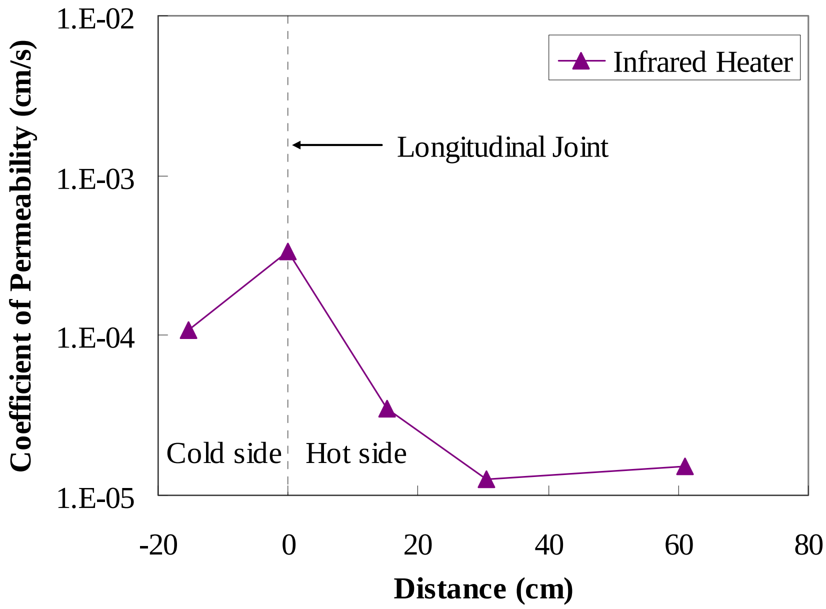


(d) Infrared Heater

Figure 4-14 Permeability Results for Project CNG155

### 4.3.3 Water Absorption

To evaluate the feasibility of the water absorption test, this test was conducted three times in this study. The average water absorption rates of replicate joint cores at each time are shown in Figure 4-15. It can be seen that the results from the three tests were consistent and repeatable. The joint cores taken from the two sealer sections (Jointbond and Replay) and the section with Pavon joint adhesive exhibited significantly lower absorption rates than the cores taken from other sections. The results indicate that joint sealers in this study were effective in preventing water from penetrating into longitudinal joint, which would help the longitudinal joint prevent moisture-related damage and make the joint perform better. One concern about joint sealer is that how long they can sustain the wear of vehicle tires. Considering that a longitudinal joint is much less often passed by vehicles than lane path, joint sealer is able to keep its effectiveness for a reasonably long period of time.

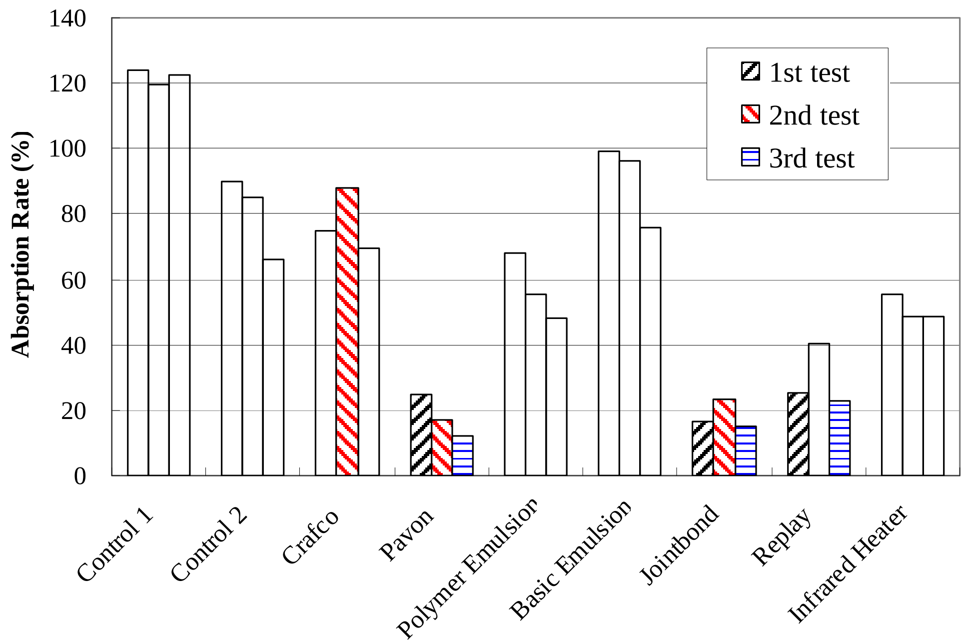


Figure 4-15 Water Absorption Rates for Project CNG155

### 4.3.4 IDT Strength

Figure 4-16 shows the indirect tensile (IDT) strength results of the field cores for the Project CNG155. It can be seen from Figure 4-16(a) that the mat on the hot side exhibited the highest IDT strength, followed by the mat on the cold side. The longitudinal joint exhibited the lowest IDT strength. This is consistent with the air void content and permeability test results. From Figure 4-16(b), polymer emulsion significantly improved IDT strength. During the construction, it was observed that Crafco joint adhesive was often picked up by the tires of haul trucks leaving the paver, which could significantly compromise its efficacy. Compared to the control sections, the IDT strength of the test sections treated with joint sealers (Jointbond and Replay) did not seem to increase at all [Figure 4-16(c)]. From Figure 4-16(d), the infrared heater was very effective in improving IDT strength, which could be attributed to the better compaction of longitudinal joint under the reheated condition.

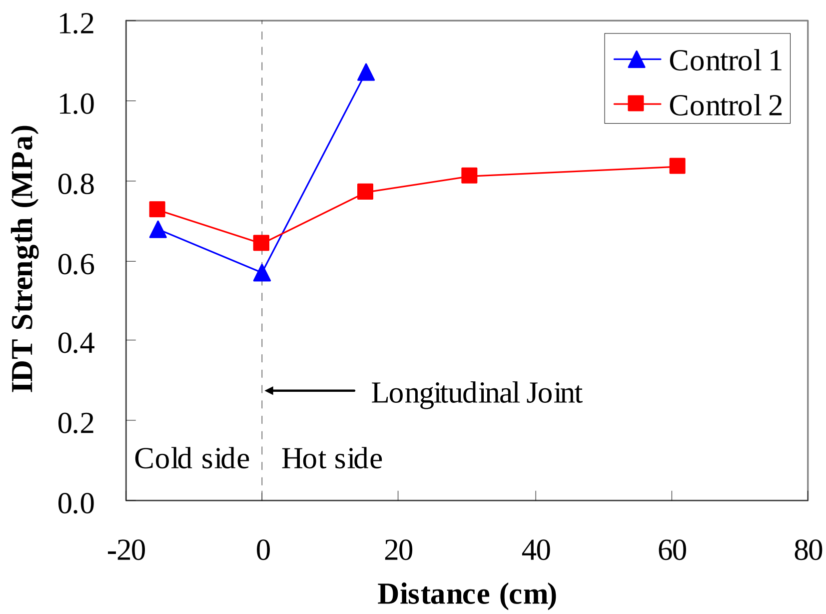


(a) Control

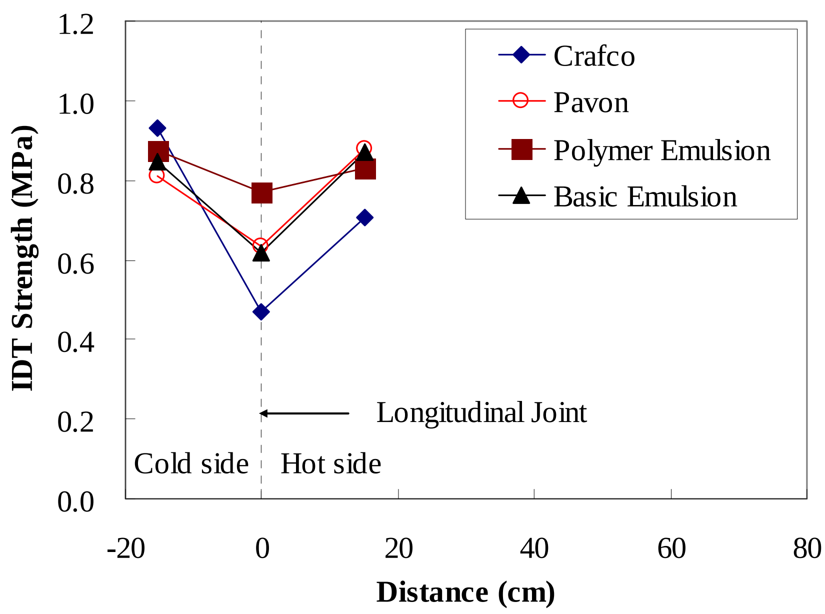


(b) Joint adhesives

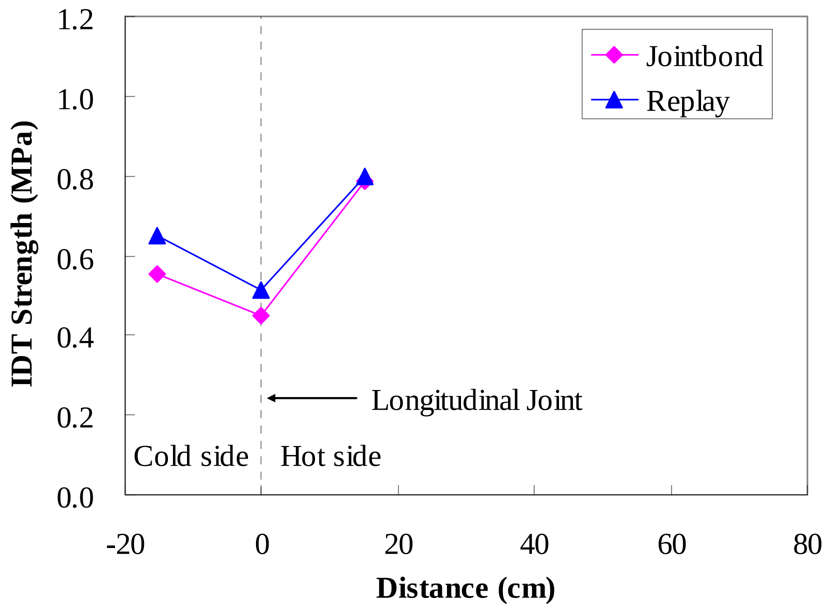


(c) Joint sealers

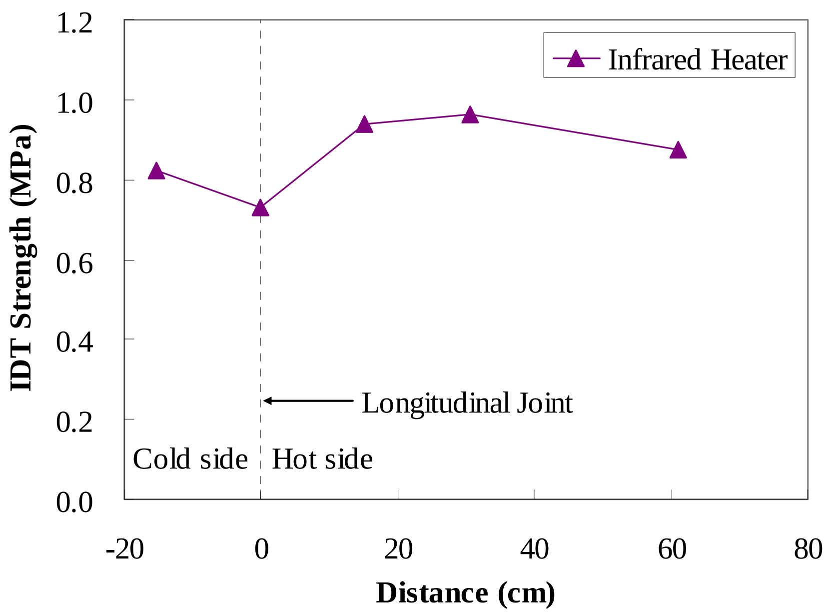


(d) Infrared heater

Figure 4-16 IDT Strength Results

### 4.3.5 X-Ray CT Analysis

Figure 4-17 presents the air void distribution of typical field cores obtained through X-ray CT image analysis. Generally, field cores exhibited high air void content near their top and bottom surfaces, and low air void content in the middle of the cores. However, the field cores taken from the joint and the mat on the cold side of the infrared heater section exhibited relatively lower air void content deep to the overlay bottom than those cores taken from the control section. This indicates that infrared heater could improve joint construction quality through increasing the compaction degree of the longitudinal joint and thus making the joint denser.

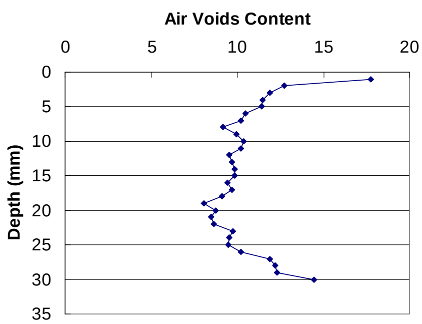


(a) Control, cold side

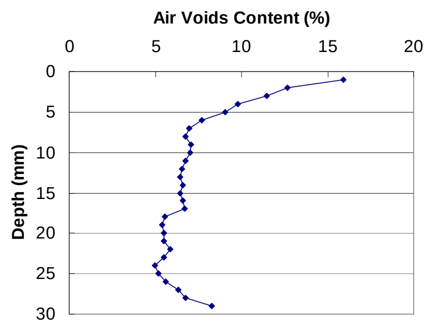


(b) Infrared heater, cold side

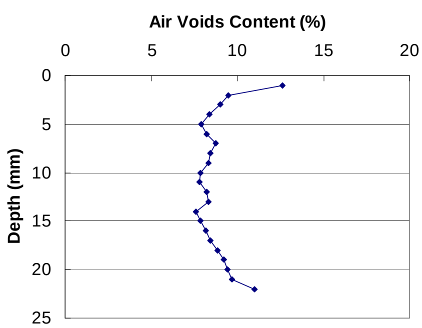


(c) Control, joint

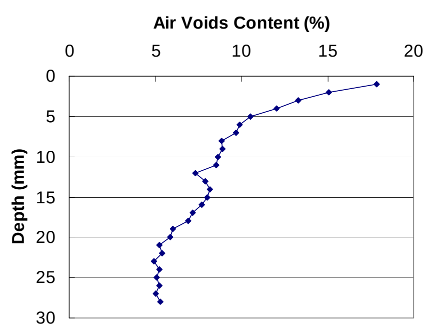


(d) Infrared heater, joint

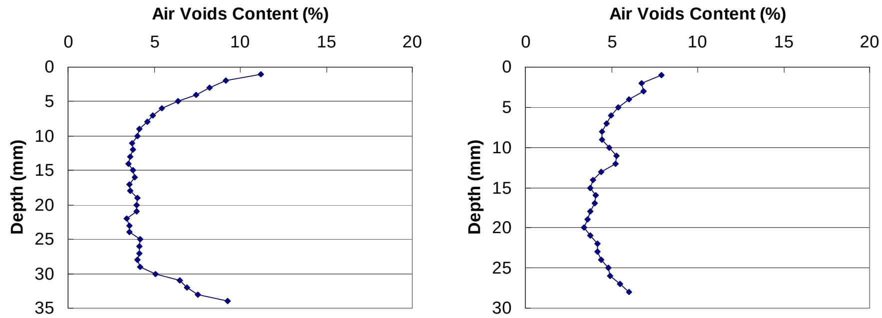


(e) Control, hot side (f) Infrared heater, hot side

Figure 4-17 Air Voids Distribution

### 4.3.6 Comparision of Different Techniques

The comparison of the different joint construction techniques used in the Project CNG155 is shown in Figure 4-18. From Figure 4-18(a), infrared heater, polymer emulsion, and basic emulsion gave the three lowest air void content. Figure 4-18(b) shows that these three techniques as well as Pavon joint adhesive gave significantly lower permeability coefficients than other joint construction techniques. In terms of IDT strength, infrared heater and polymer emulsion gave two highest strength values among all the techniques evaluated. Overall, joint heater performed best among the techniques because it yielded low air void content and permeability, and high IDT strength. This is consistent with the findings from other studies about joint heater (Daniel and Real 2006; Fleckenstein et al. 2002). In addition, some of the joint adhesives performed well (such as polymer emulsion) in terms of IDT strength. However, the joint sealers used in the study did not significantly reduce water permeability as expected, but they did reduce water absorption rates, which may still suggest a good durability performance for longitudinal joint.

It should be noted that the overlay used in this study was 31.8 cm (1.25 in.) thick. The effectiveness of joint heater may be compromised with the increase in the layer thickness because infrared may not be able to penetrate through the thick layer to heat the asphalt mixture at the bottom. Unlike infrared heater, joint adhesive is applied right along longitudinal joint and joint sealer is spray applied on pavement surface along longitudinal joint after construction, their effectiveness should have nothing to do with the thickness of pavement layer.

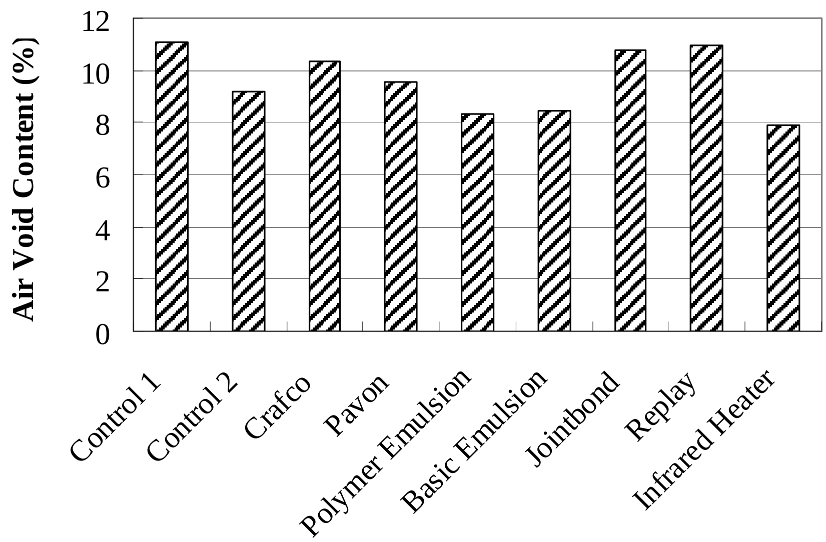


(a) Air Void Content

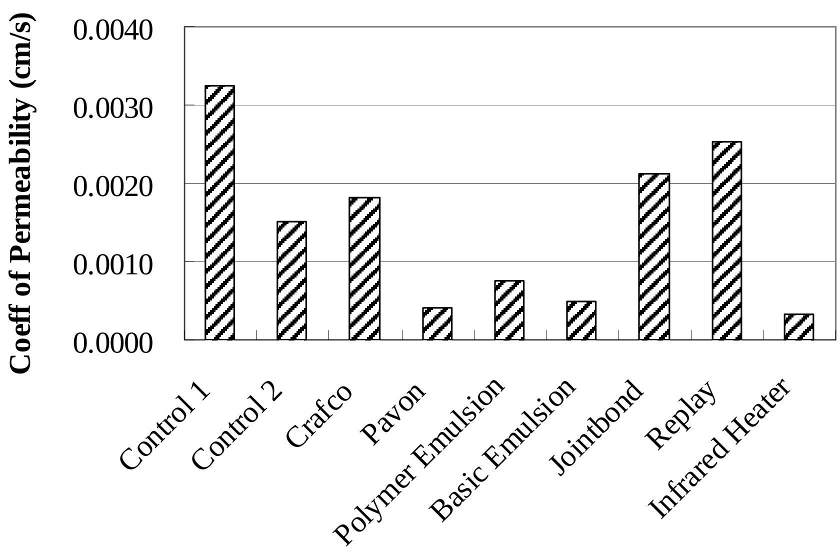


(b) Permeability

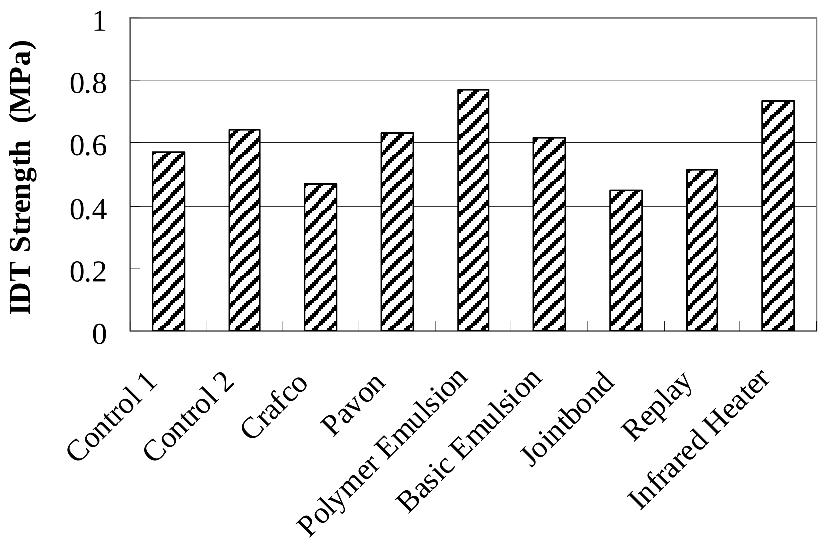


(c) IDT Strength

Figure 4-18 Comparison of Different Joint Construction Techniques

# CHAPTER 5 TENNESSEE LONGITUDINAL JOINT SURVEY

## 5.1 Introduction

Longitudinal joint cracking is one of the major distresses for asphalt pavements. The cracks occurred along longitudinal joints compromise the integrity of asphalt pavements and aggravate other forms of asphalt pavement distress, such as raveling and moisture damage. The cracks will eventually pose a major danger to traffic safety. It is essential to obtain the information on longitudinal joint condition for making decision on asphalt pavement maintenance.

This survey utilizes the Highway Pavement Management Application (HPMA) system to summarize the longitudinal joint cracking results of interstate highways and state routes of Tennessee and provide an overall evaluation of the longitudinal joint condition in Tennessee.

## 5.2 Survey on the Longitudinal Joint Condition of Interstate Highways in Tennessee

Thirteen interstates in Tennessee were evaluated about their longitudinal joint cracking conditions based on the data retrieved from HPMA system. Their longitudinal joint cracking performance in 2007 is summarized in Table 5-1. The longitudinal joint cracking in the HPMA system is categorized into three types based on the severity level: low, moderate, and high.

Table 5-1 Longitudinal Joint Cracking on the Interstates of Tennessee in 2007

| Interstate | Total Damage (mile) | | | Center-Line Length (mile) | Cracking Percentage | | |
|---|---|---|---|---|---|---|---|
| | Low | Moderate | High | | Low | Moderate | High |
| I-24 | 0.251 | 0.03 | 0.008 | 185 | 0.0678 | 0.0081 | 0.00216 |
| I-26 | 0.181 | 0.009 | 0 | 70 | 0.1293 | 0.0064 | 0 |
| I-40 | 1.769 | 0.181 | 0.018 | 451 | 0.1961 | 0.0201 | 0.00200 |
| I-55 | 0.084 | 0.009 | 0.001 | 12 | 0.3500 | 0.0375 | 0.00417 |
| I-65 | 0.281 | 0.027 | 0.006 | 117 | 0.1201 | 0.0115 | 0.00256 |
| I-75 | 0.209 | 0.009 | 0.001 | 160 | 0.0653 | 0.0028 | 0.00031 |
| I-81 | 0.062 | 0.016 | 0.001 | 74 | 0.0419 | 0.0108 | 0.00068 |
| I-140 | 0.221 | 0 | 0 | 14 | 0.7893 | 0 | 0 |
| I-155 | 0.254 | 0.003 | 0 | 15 | 0.8467 | 0.0100 | 0 |
| I-240 | 0.6 | 0.066 | 0.002 | 32 | 0.9375 | 0.1031 | 0.00313 |
| I-275 | 0.032 | 0.003 | 0 | 3 | 0.5333 | 0.0500 | 0 |
| I-440 | 0.005 | 0 | 0 | 7 | 0.0357 | 0 | 0 |
| I-640 | 0.017 | 0 | 0 | 8 | 0.1063 | 0 | 0 |
| Average | | | | | 0.3246 | 0.0200 | 0.0012 |
| Standard Deviation | | | | | 0.3353 | 0.0291 | 0.0015 |

### 5.2.1 Overall Cracking Performance of Interstates in Tennessee

Table 5-1 and Figure 5-1 present the overall cracking performance of the interstates of Tennessee in 2007. The average cracking percentage of all thirteen interstates in Tennessee was less than 0.35% at low severity level, i.e. less than 5.6 meters out of 1 mile of interstate pavement exhibited the low level cracking. From Table 5-1 and Figure 5-1, it is also observed that much less of Tennessee interstates experienced the moderate and high level cracking. This indicates that the overall longitudinal joint on interstates performed well in Tennessee.

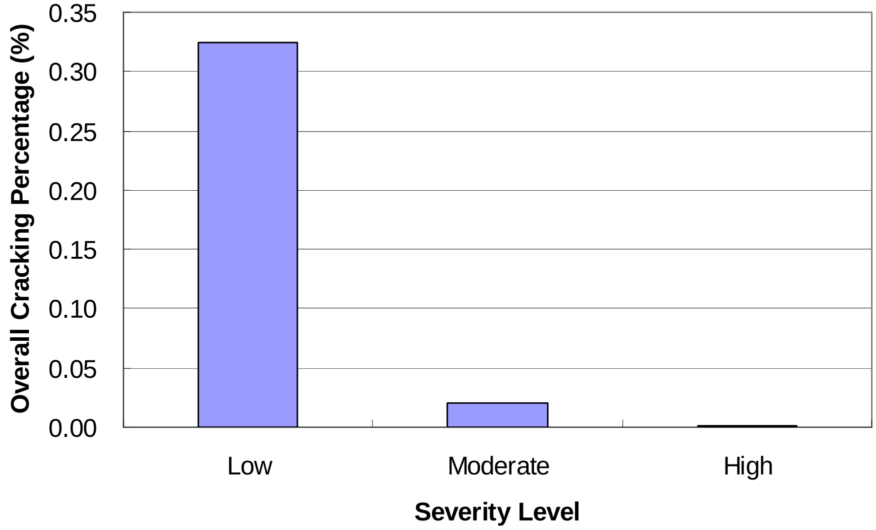


Figure 5-1 Cracking Performance of Interstates in Tennessee

### 5.2.2 Interstate 40

The Interstate 40 is a major interstate east-west route going through Tennessee. The cracking condition of I-40 is shown in Figure 5-2. The total cracking length at low severity level on I-40 was about 1.8 miles, less than 0.2% of its total length in Tennessee. The total length and overall percentage for moderate and severe cracking were much less compared to the low cracking level.

### 5.2.3 Comparison of East-West Interstate Routes

Figure 5-3 presents the comparison of three east-west interstate highway routes in Tennessee. It can be seen that I-40 had the longest total cracked longitudinal joint than the other two interstates (I-24 and I-26) because it has the longest mileage in Tennessee. In terms of overall cracking percentage, the longitudinal joint on I-40 performed worst among the three interstate routes.

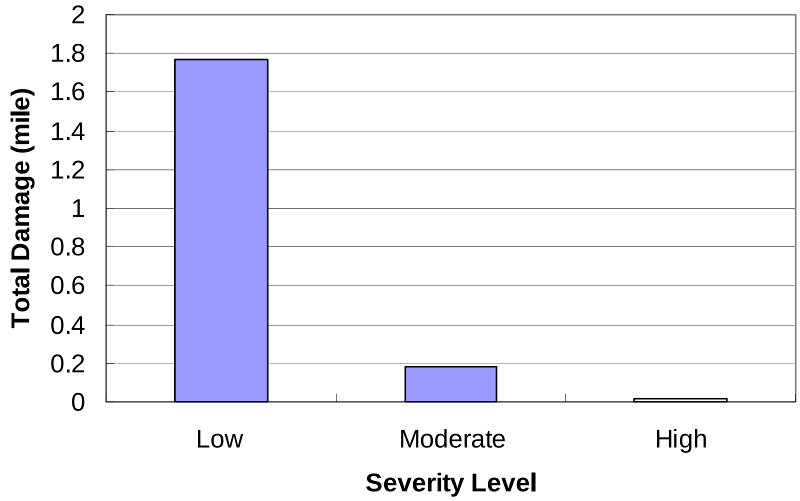


(a) Total Damage

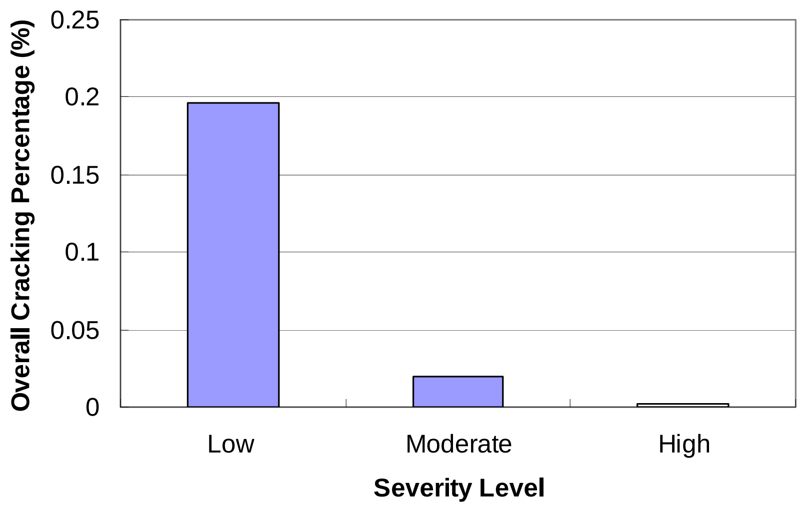


(b) Overall Cracking Percentage

Figure 5-2 Longitudinal Joint Cracking on Interstate 40

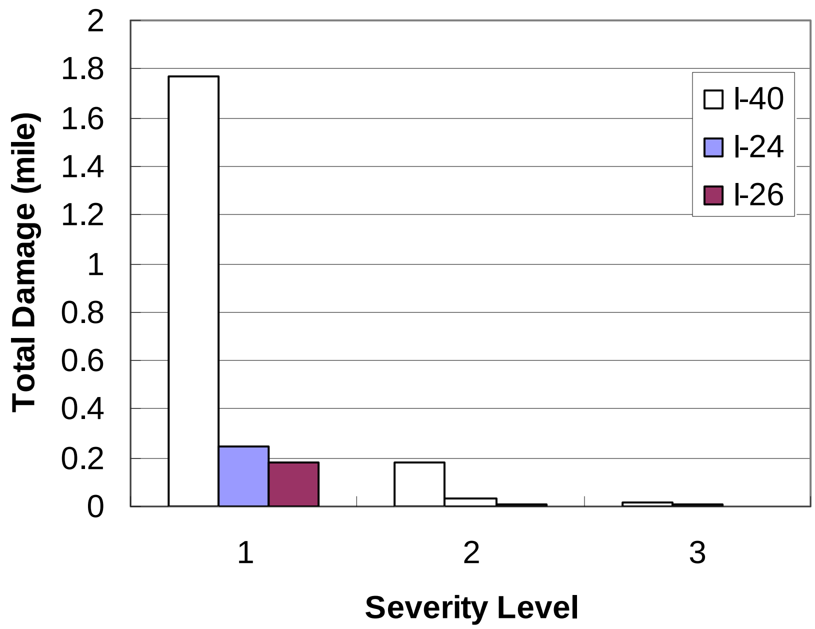


(a) Total Damage

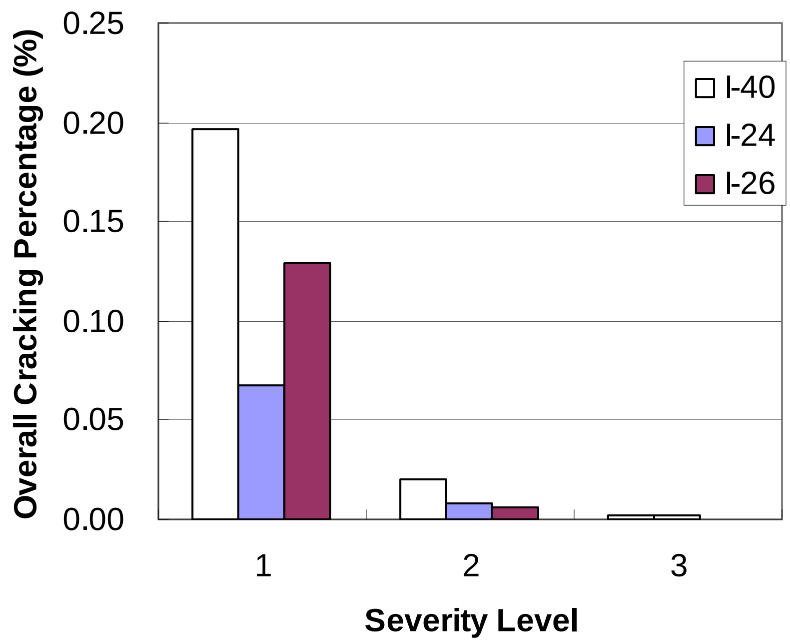


(b) Overall Cracking Percentage

Figure 5-3 Comparison of East-West Interstate Routes

### 5.2.4 Comparison of North-South Interstate Routes

Figure 5-4 presents the comparison of four north-south interstate highway routes in Tennessee. It can be seen that the three major north-west interstate routes in Tennessee (I-65, I-75, and I-81) were subjected to similar longitudinal joint failure in terms of both total crack length and overall cracking percentage, among which I-81 performed the best and I-65 performed the worst.

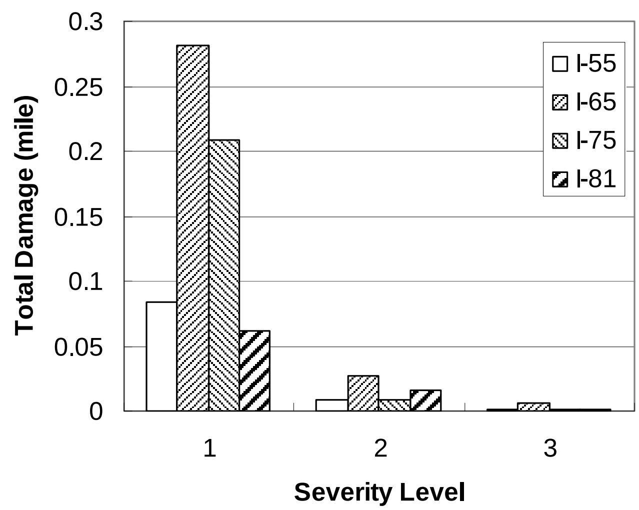


(a) Total Damage

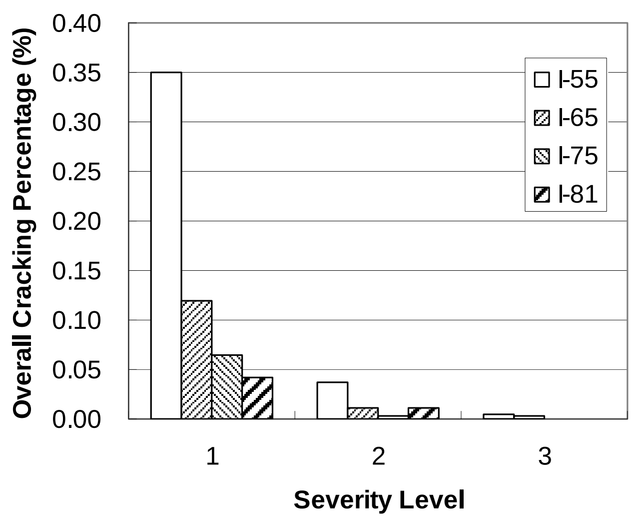


(b) Overall Cracking Percentage

Figure 5-4 Comparison of North-West Interstate Routes

### 5.2.5 Longitudinal Joint Cracking on Auxiliary Interstate Routes

Figure 5-5 presents the longitudinal joint cracking on auxiliary interstate routes in Tennessee at the low severity level. It can be seen that the ranking of the longitudinal joint performance was similar based on total crack length and overall cracking performance.

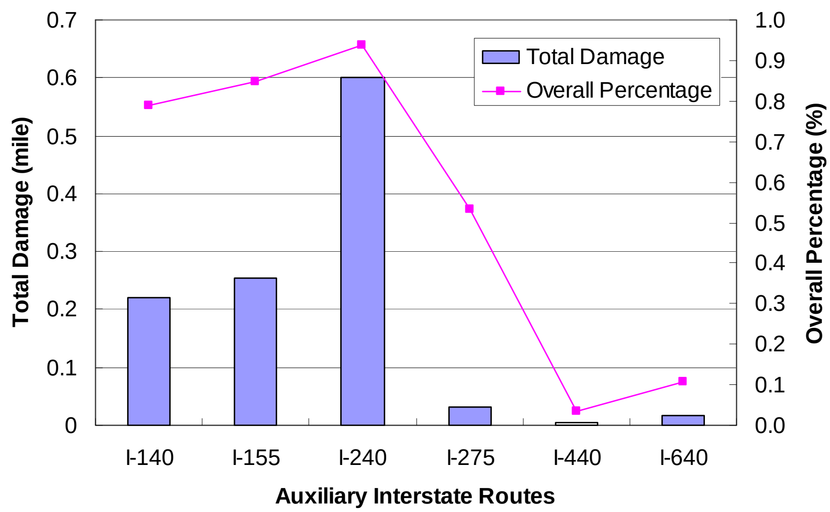


Figure 5-5 Longitudinal Joint Cracking on Auxiliary Interstate Routes

## 5.3 Survey on the Longitudinal Joint Condition of State Routes in Tennessee

Almost 400 states routes of Tennessee were evaluated about their longitudinal joint cracking performance. Since the state routes are surveyed every two years in Tennessee, the longitudinal joint cracking performance in either 2006 or 2007 of the Tennessee state routes is summarized in Table A-1 of the Appendix. Figure 5-6 presents the comparison of longitudinal joint performance in 2006 and 2007. Figure 5-7 presents the overall cracking performance of major Tennessee state routes with center-line length equal to or greater than 10 miles. The distributions of the longitudinal joint cracking performance of major state routes and their distribution parameters were presented in Table 5-2 and Figure 5-8.

It is observed from Figure 5-6 that the state routes in Tennessee experienced more cracking in 2007 than in 2006. Major state routes with center-line length ≥ 10 miles were selected for the evaluation of the overall cracking performance of longitudinal joint on Tennessee state routes. Figure 5-7 shows that the cracking pattern of the major state routes at different severity levels similar to that in Figure 5-1 for the interstates in Tennessee. However, cracking percentage values show that the state routes exhibited much worse cracking than the interstates in Tennessee. At the low severity level, Tennessee Interstate highways exhibited less than 0.35% cracking, whereas state routes experienced 0.8% cracking. This indicated the longitudinal joints on the state routes in Tennessee did not perform so good as on the Interstate highways.

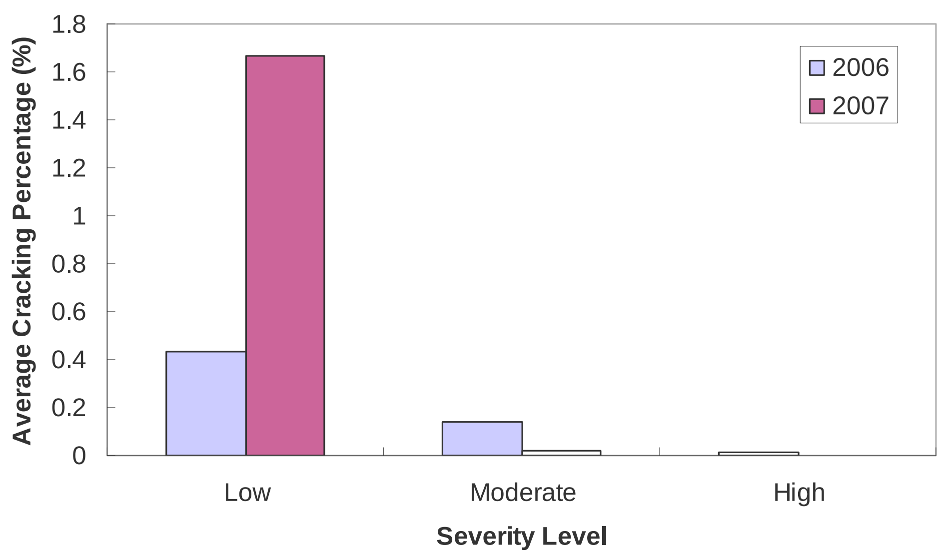


Figure 5-6 Comparison of Longitudinal Joint Cracking on Tennessee State Routes

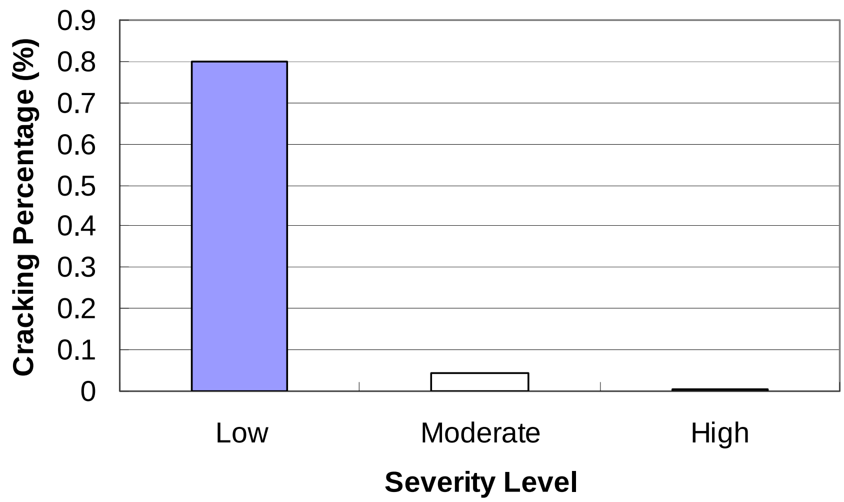


Figure 5-7 Cracking Performance of Major Tennessee State Routes
(Center-length ≥ 10 miles)

From Table 5-3 and Figure 5-8, it can be seen that almost 80% of the state routes in Tennessee experienced less than 1% cracking at the low severity level. At the moderate and high severity levels, almost 40% and 80% of the state routes experienced no cracking at all. Only a relatively small percentages of the state route experienced cracking at three different severity levels.

Table 5-3 Distribution Parameters of Longitudinal Joint Cracking Percentage on Major Tennessee State Routes (%)

| Parameters | | Severity Level | | |
|---|---|---|---|---|
| | | Low | Moderate | High |
| Quantiles | 100% | 8.2992 | 0.8432 | 0.0819 |
| | 90% | 2.2150 | 0.1515 | 0.0067 |
| | 75% | 0.9448 | 0.0275 | 0 |
| | 50% | 0.3510 | 0.0058 | 0 |
| | 25% | 0.0942 | 0 | 0 |
| | 10% | 0.0333 | 0 | 0 |
| | 0% | 0 | 0 | 0 |
| Mean | | 0.7995 | 0.0423 | 0.0023 |
| Std Dev | | 1.1997 | 0.0998 | 0.0080 |

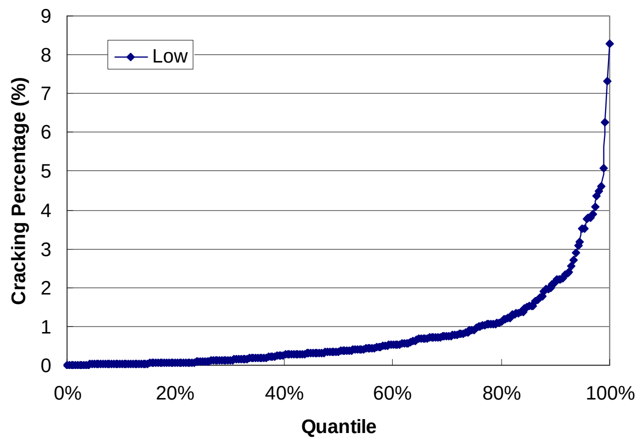


**(a) Low Severity Level**

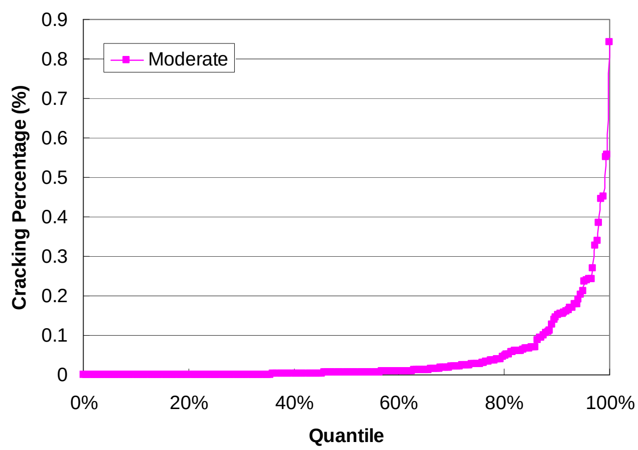


**(b) Moderate Severity Level**

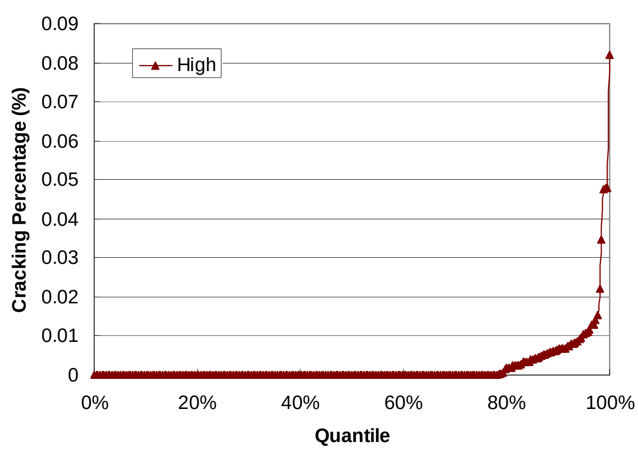


**(c) High Severity Level**

Figure 5-8 Distribution of Longitudinal Joint Cracking Percentage of Major Tennessee State Routes

# CHAPTER 6 CONCLUSIONS

Field cores from three projects constructed with different longitudinal joint construction techniques were tested in the laboratory to compare and evaluate the effectiveness of these techniques in improving the joint performance. The laboratory tests included air void content, permeability, indirect tensile (IDT) strength, water absorption, and X-ray CT tests. Seven longitudinal joint products were evaluated, which can be categorized into three types of construction techniques: joint adhesives (Crafco, Pavon, polymer emulsion and basic emulsion commonly used by TDOT), joint sealers (Jointbond and Replay), and infrared joint heater. Based on the results from this study, the following conclusions can be summarized:

- Air voids, permeability, and IDT strength of field cores show general consistency in characterizing the construction quality of longitudinal joint, i.e., the lower the air void content, the lower the permeability, and the higher the IDT strength.
- The longitudinal joint constructed without any special technique exhibited higher air void content, higher permeability, and lower IDT strength than its neighboring area on cold and hot side. This indicates that longitudinal joint construction quality may not be guaranteed with conventional construction practice. It is recommended that special joint construction techniques be adopted to improve the construction quality of longitudinal joints in asphalt pavements.
- Without special joint construction techniques, the mat on the cold side exhibited higher air void content, higher permeability, and lower IDT strength than the mat on the hot side. The can be attributed to the difference in the compaction. The mat on the cold side is compacted under unconfined state whereas the mat on the hot side is compacted under confined state (confined by the cold side).
- Among the four joint adhesives used in this study, only polymer emulsion appeared

to increase the IDT strength of longitudinal joint. The efficacy of Crafco joint adhesive may be compromised during construction because it was picked up by the tires of haul trucks leaving the paver.

- The results from the ordinary falling head permeability test show that the joint sealers used in this study did not reduce the permeability of the field cores. The reason may lie in the fact that the sealant membrane was not so strong as to withstand the relatively high water head in the permeability test. However, the results from the water absorption test indicate that joint sealers may be still effective in preventing water from penetrating into pavement joint through the reduced water absorption rates.
- The infrared heater exhibited the best performance among all the joint construction techniques evaluated in the study. The infrared heater was effective in reducing air void content and water permeability, and increasing IDT strength.
- The air voids distribution obtained from the X-ray CT images shows that the effectiveness of infrared heater in improving joint quality was through increasing the compaction degree of longitudinal joint deep to the overlay bottom and thus making the joint denser.
- The Tennessee longitudinal joint survey shows that the overall longitudinal joints on the interstates of Tennessee performed well, whereas the state routes exhibited much worse longitudinal cracking.

# REFERENCES


Buchanan, M. S. (2000). “Evaluation of Notched Wedge Longitudinal Joint Construction.” Transportation Research Record 1712, Transportation Research Board, Washington, D.C., 50–57.

Burati, J.L., Jr., and G.B. Elzoghbi (1987). “Study of Joint Densities in Bituminous Airport Pavements.” Transportation Research Record 1126, TRB, National Research Council, Washington, DC.

Daniel, J. S. and Real, W. L. (2006). "Field Trial of Infrared Joint Heater to Improve Longitudinal Joint Performance in New Hampshire." Transportation Research Record 1946, Transportation Research Board, Washington, D.C., 157–162.

Estakhri, C., T.J. Freeman, and C. Spiegelman (2001). “Density Evaluation of the Longitudinal Construction Joint of Hot-Mix Asphalt Pavements.” Report. 1757. Texas Transportation Institute, College Station, TX.

Fleckenstein, L.J., Allen, D.L., and Schultz, D.B. (2002). “Compaction at the Longitudinal Construction Joint in Asphalt Pavements.” Report No. KTC - 02 -10/SPR 208-00-1F, Kentucky Transportation Center, Univ. of Kentucky, Lexington, KY.

Foster, C.R., S.B. Hudson, and R.S. Nelson (1964). “Constructing Longitudinal Joints in Hot Mix Asphalt Pavements.” Highway Research Record 51, TRB, National Research Council, Washington, DC.

Kandhal, P. S., and Mallick, R. B. (1996a). “A Study of Longitudinal Joint Construction Techniques in HMA Pavements (Interim Report—Colorado project).” NCAT Rep. No. 96-3, National Center for Asphalt Technology (NCAT), Auburn Univ., Auburn, Ala.

Kandhal, P. S., and Mallick, R. B. (1996b). “Study of Longitudinal Joint Construction Techniques in Hot-Mix Asphalt Pavements.” Transportation Research Record 1543, Transportation Research Board, Washington, D.C., 106–112.

Kandhal, P. S., and Mallick, R. B. (1997a). “Longitudinal Joint Construction Techniques for Asphalt Pavements.” NCAT Rep. No. 97-4, National Center for Asphalt Technology NCAT , Auburn Univ., Auburn, Ala.

Kandhal, P. S., and Mallick, R. B. (1997b). “Longitudinal Joint Construction Techniques for Asphalt Pavements.” Proc., 8th Int. Conf. on Asphalt Pavements, Vol. 1, Univ. of Washington, Seattle.

Kandhal, P. S., and Mallick, R. B. (2007). “Evaluation of Various Longitudinal Joint Construction Techniques for Asphalt Airport Pavements.” 2007 FAA Worldwide Airport Technology Transfer Conference, Atlantic City, New Jersey.

Kandhal, P. S., Ramirez, T. L., and Ingram, P. M. (2002). “Evaluation of Eight Longitudinal Joint Construction Techniques for Asphalt Pavements in Pennsylvania.” NCAT Rep. No. 2002-03, National Center for Asphalt Technology NCAT , Auburn Univ., Auburn, Ala.

Kandhal, P. S., and Rao, S. S. (1994a). “Evaluation of Longitudinal Joint Construction Techniques for Asphalt Pavements.” NCAT Rep. No. 94-1, National Center for Asphalt Technology NCAT , Auburn Univ., Auburn, Ala.

Kandhal, P. S., and Rao, S. (1994b). “Evaluation of Longitudinal Joint Construction Techniques for Asphalt Pavements.” Transportation Research Record 1469, Transportation Research Board, Washington, D.C.

Livneh, M. (1988). “Site and Laboratory Testing in Order to Determine the Bonding Method in Construction Joints of Asphalt Strip.” Proceedings, AAPT, Vol. 57.

Toepel, A. (2003). “Evaluation of Techniques for Asphaltic Pavement Longitudinal Joint Construction.” Report No. WI-08-03, Wisconsin Department of Transportation, Madison, WI.

# APPENDIX

## Longitudinal Joint Cracking on the State Routes of Tennessee

Table A-1 Longitudinal Joint Cracking on the State Routes of Tennessee

| State Route | Total Damage (mile) | | | Center-Line Length (mile) | Cracking Percentage | | | Year |
|---|---|---|---|---|---|---|---|---|
| | Low | Moderate | High | | Low | Moderate | High | |
| SR-1 | 4.057 | 0.035 | 0.001 | 270.6 | 1.4993 | 0.0129 | 0.0004 | 2007 |
| SR-2 | 0.452 | 0 | 0 | 168.8 | 0.2678 | 0 | 0 | 2007 |
| SR-3 | 2.401 | 0.072 | 0.001 | 137.6 | 1.7449 | 0.0523 | 0.0007 | 2007 |
| SR-4 | 0.58 | 0.016 | 0.001 | 14.9 | 3.8926 | 0.1074 | 0.0067 | 2007 |
| SR-5 | 4.222 | 0.243 | 0.008 | 120.4 | 3.5066 | 0.2018 | 0.0066 | 2007 |
| SR-6 | 0.455 | 0.008 | 0 | 150.8 | 0.3017 | 0.0053 | 0 | 2007 |
| SR-7 | 0.043 | 0 | 0 | 81 | 0.0531 | 0 | 0 | 2007 |
| SR-10 | 0.126 | 0.008 | 0 | 132 | 0.0955 | 0.0061 | 0 | 2007 |
| SR-11 | 1.136 | 0.009 | 0 | 144.7 | 0.7851 | 0.0062 | 0 | 2007 |
| SR-12 | 0.199 | 0.006 | 0.002 | 57.9 | 0.3437 | 0.0104 | 0.0035 | 2007 |
| SR-13 | 0.547 | 0.009 | 0 | 151.9 | 0.3601 | 0.0059 | 0 | 2007 |
| SR-14 | 0.565 | 0.025 | 0.008 | 56.5 | 1.0000 | 0.0442 | 0.0142 | 2007 |
| SR-15 | 3.049 | 0.05 | 0.001 | 228 | 1.3373 | 0.0219 | 0.0004 | 2007 |
| SR-16 | 1.804 | 0.063 | 0 | 40.1 | 4.4988 | 0.1571 | 0 | 2007 |
| SR-18 | 0.352 | 0.008 | 0 | 46.5 | 0.7570 | 0.0172 | 0 | 2007 |
| SR-19 | 0.813 | 0.012 | 0 | 42.9 | 1.8951 | 0.0280 | 0 | 2007 |
| SR-20 | 0.424 | 0.005 | 0 | 143.5 | 0.2955 | 0.0035 | 0 | 2007 |
| SR-21 | 0.244 | 0.002 | 0 | 34.1 | 0.7155 | 0.0059 | 0 | 2007 |
| SR-22 | 1.957 | 0.008 | 0 | 187.1 | 1.0460 | 0.0043 | 0 | 2007 |
| SR-23 | 0.302 | 0.006 | 0.001 | 8.9 | 3.3933 | 0.0674 | 0.0112 | 2007 |
| SR-24 | 0.283 | 0 | 0 | 75.1 | 0.3768 | 0 | 0 | 2007 |
| SR-25 | 0.182 | 0.001 | 0 | 59.7 | 0.3049 | 0.0017 | 0 | 2007 |
| SR-26 | 0.019 | 0 | 0 | 39.1 | 0.0486 | 0 | 0 | 2007 |
| SR-41 | 0.157 | 0 | 0 | 22.9 | 0.6856 | 0 | 0 | 2007 |
| SR-43 | 0.695 | 0.001 | 0 | 57.1 | 1.2172 | 0.0018 | 0 | 2007 |
| SR-45 | 0.048 | 0 | 0 | 18 | 0.2667 | 0.0000 | 0 | 2007 |
| SR-46 | 0.423 | 0.001 | 0 | 74.9 | 0.5648 | 0.0013 | 0 | 2007 |
| SR-47 | 0.079 | 0 | 0 | 19.8 | 0.3990 | 0 | 0 | 2007 |
| SR-48 | 0.48 | 0.003 | 0 | 93.1 | 0.5156 | 0.0032 | 0 | 2007 |
| SR-49 | 0.47 | 0.016 | 0 | 104.8 | 0.4485 | 0.0153 | 0 | 2007 |
| SR-50 | 0.451 | 0.005 | 0 | 113.1 | 0.3988 | 0.0044 | 0 | 2007 |
| SR-52 | 0.102 | 0.005 | 0 | 91.4 | 0.1116 | 0.0055 | 0 | 2007 |
| SR-53 | 0.001 | 0 | 0 | 101.1 | 0.0010 | 0 | 0 | 2007 |
| SR-54 | 1.592 | 0.1 | 0.012 | 115 | 1.3843 | 0.0870 | 0.0104 | 2007 |
| SR-55 | 0.013 | 0 | 0 | 37.1 | 0.0350 | 0 | 0 | 2007 |

Table A-1 Longitudinal Joint Cracking on the State Routes of Tennessee (Cont'd)

| State Route | Total Damage (mile) | | | Center-Line Length (mile) | Cracking Percentage | | | Year |
|---|---|---|---|---|---|---|---|---|
| | Low | Moderate | High | | Low | Moderate | High | |
| SR-56 | 0.027 | 0 | 0 | 128.7 | 0.0210 | 0 | 0 | 2007 |
| SR-57 | 1.175 | 0.005 | 0 | 110.1 | 1.0672 | 0.0045 | 0 | 2007 |
| SR-59 | 2.868 | 0.027 | 0.002 | 45.9 | 6.2484 | 0.0588 | 0.0044 | 2007 |
| SR-64 | 0.271 | 0.001 | 0 | 34.3 | 0.7901 | 0.0029 | 0 | 2007 |
| SR-65 | 0.061 | 0 | 0 | 32.4 | 0.1883 | 0 | 0 | 2007 |
| SR-69 | 2.633 | 0.015 | 0 | 173.1 | 1.5211 | 0.0087 | 0 | 2007 |
| SR-76 | 6.632 | 0.022 | 0 | 208.3 | 3.1839 | 0.0106 | 0 | 2007 |
| SR-77 | 1.083 | 0.001 | 0 | 65 | 1.6662 | 0.0015 | 0 | 2007 |
| SR-78 | 1.474 | 0.025 | 0.004 | 36 | 4.0944 | 0.0694 | 0.0111 | 2007 |
| SR-79 | 0.007 | 0 | 0 | 10.4 | 0.0673 | 0 | 0 | 2007 |
| SR-80 | 0.031 | 0 | 0 | 14.1 | 0.2199 | 0 | 0 | 2007 |
| SR-82 | 0.079 | 0 | 0 | 25 | 0.3160 | 0 | 0 | 2007 |
| SR-87 | 0.821 | 0.026 | 0 | 39.3 | 2.0891 | 0.0662 | 0 | 2007 |
| SR-88 | 0.675 | 0.016 | 0 | 41.1 | 1.6423 | 0.0389 | 0 | 2007 |
| SR-89 | 3.69 | 0.003 | 0.004 | 50.5 | 7.3069 | 0.0059 | 0.0079 | 2007 |
| SR-96 | 0.198 | 0.002 | 0 | 76.8 | 0.2578 | 0.0026 | 0 | 2007 |
| SR-98 | 0.005 | 0 | 0 | 11.8 | 0.0424 | 0.0000 | 0 | 2007 |
| SR-99 | 0.328 | 0.003 | 0 | 117.7 | 0.2787 | 0.0025 | 0 | 2007 |
| SR-100 | 1.408 | 0.008 | 0 | 130.8 | 1.0765 | 0.0061 | 0 | 2007 |
| SR-102 | 0.005 | 0 | 0 | 13.1 | 0.0382 | 0 | 0 | 2007 |
| SR-103 | 0.004 | 0 | 0 | 8.4 | 0.0476 | 0 | 0 | 2007 |
| SR-104 | 2.09 | 0.012 | 0 | 98.9 | 2.1132 | 0.0121 | 0 | 2007 |
| SR-105 | 0.242 | 0.001 | 0 | 44.5 | 0.5438 | 0.0022 | 0 | 2007 |
| SR-106 | 0.205 | 0.003 | 0 | 53.4 | 0.3839 | 0.0056 | 0 | 2007 |
| SR-109 | 0.036 | 0 | 0.001 | 38.6 | 0.0933 | 0.0000 | 0.0026 | 2007 |
| SR-110 | 0.068 | 0 | 0 | 22.6 | 0.3009 | 0 | 0 | 2007 |
| SR-112 | 1.288 | 0.005 | 0 | 41.9 | 3.0740 | 0.0119 | 0 | 2007 |
| SR-114 | 0.865 | 0.007 | 0 | 85.8 | 1.0082 | 0.0082 | 0 | 2007 |
| SR-117 | 0.807 | 0.001 | 0 | 6.4 | 12.6094 | 0.0156 | 0 | 2007 |
| SR-118 | 0.357 | 0 | 0 | 14.8 | 2.4122 | 0 | 0 | 2007 |
| SR-119 | 0.043 | 0 | 0 | 4.7 | 0.9149 | 0 | 0 | 2007 |
| SR-120 | 0.129 | 0 | 0 | 12.2 | 1.0574 | 0 | 0 | 2007 |
| SR-121 | 0.013 | 0 | 0 | 11.5 | 0.1130 | 0 | 0 | 2007 |
| SR-124 | 0.97 | 0.005 | 0.001 | 19.1 | 5.0785 | 0.0262 | 0.0052 | 2007 |
| SR-125 | 0.877 | 0.032 | 0 | 34.4 | 2.5494 | 0.0930 | 0 | 2007 |

Table A-1 Longitudinal Joint Cracking on the State Routes of Tennessee (Cont'd)

| State Route | Total Damage (mile) | | | Center-Line Length (mile) | Cracking Percentage | | | Year |
|---|---|---|---|---|---|---|---|---|
| | Low | Moderate | High | | Low | Moderate | High | |
| SR-128 | 0.159 | 0.003 | 0 | 45.3 | 0.3510 | 0.0066 | 0 | 2007 |
| SR-129 | 0.109 | 0.002 | 0 | 45.3 | 0.2406 | 0.0044 | 0 | 2007 |
| SR-130 | 0.05 | 0.004 | 0 | 28.7 | 0.1742 | 0.0139 | 0 | 2007 |
| SR-138 | 0.253 | 0.039 | 0.008 | 23.1 | 1.0952 | 0.1688 | 0.0346 | 2007 |
| SR-140 | 0.947 | 0.003 | 0 | 40.4 | 2.3441 | 0.0074 | 0 | 2007 |
| SR-141 | 0.263 | 0 | 0 | 51.9 | 0.5067 | 0 | 0 | 2007 |
| SR-142 | 0.168 | 0.004 | 0 | 22.2 | 0.7568 | 0.0180 | 0 | 2007 |
| SR-147 | 0.068 | 0.001 | 0 | 23 | 0.2957 | 0.0043 | 0 | 2007 |
| SR-149 | 0.006 | 0 | 0 | 21.9 | 0.0274 | 0 | 0 | 2007 |
| SR-151 | 0.035 | 0 | 0 | 4.9 | 0.7143 | 0 | 0 | 2007 |
| SR-155 | 0.104 | 0.007 | 0.002 | 29.7 | 0.3502 | 0.0236 | 0.0067 | 2007 |
| SR-157 | 0.68 | 0 | 0.001 | 5.3 | 12.8302 | 0 | 0.0189 | 2007 |
| SR-161 | 0.001 | 0 | 0 | 10 | 0.0100 | 0 | 0 | 2007 |
| SR-166 | 0.388 | 0.002 | 0 | 47.1 | 0.8238 | 0.0042 | 0 | 2007 |
| SR-171 | 0.151 | 0.001 | 0 | 18 | 0.8389 | 0.0056 | 0 | 2007 |
| SR-174 | 0.02 | 0.001 | 0 | 40.8 | 0.0490 | 0.0025 | 0 | 2007 |
| SR-175 | 0.085 | 0.003 | 0 | 25.2 | 0.3373 | 0.0119 | 0 | 2007 |
| SR-176 | 0.022 | 0.002 | 0 | 6 | 0.3667 | 0.0333 | 0 | 2007 |
| SR-177 | 0.298 | 0.001 | 0 | 13.2 | 2.2576 | 0.0076 | 0 | 2007 |
| SR-178 | 0.054 | 0 | 0 | 11.6 | 0.4655 | 0 | 0 | 2007 |
| SR-179 | 0.213 | 0.003 | 0 | 38.5 | 0.5532 | 0.0078 | 0 | 2007 |
| SR-180 | 0.062 | 0 | 0 | 12.6 | 0.4921 | 0 | 0 | 2007 |
| SR-181 | 0.502 | 0 | 0 | 25.1 | 2.0000 | 0 | 0 | 2007 |
| SR-182 | 0.114 | 0 | 0 | 9.8 | 1.1633 | 0 | 0 | 2007 |
| SR-183 | 0.17 | 0.003 | 0 | 14.2 | 1.1972 | 0.0211 | 0 | 2007 |
| SR-184 | 0.438 | 0 | 0 | 11.6 | 3.7759 | 0 | 0 | 2007 |
| SR-185 | 0.179 | 0.013 | 0 | 7.7 | 2.3247 | 0.1688 | 0 | 2007 |
| SR-186 | 0.26 | 0.005 | 0.002 | 25.5 | 1.0196 | 0.0196 | 0.0078 | 2007 |
| SR-187 | 0.16 | 0 | 0 | 7.9 | 2.0253 | 0 | 0 | 2007 |
| SR-188 | 0.219 | 0.001 | 0 | 22.4 | 0.9777 | 0.0045 | 0 | 2007 |
| SR-189 | 0.223 | 0 | 0 | 5.4 | 4.1296 | 0 | 0 | 2007 |
| SR-190 | 0.423 | 0.005 | 0.001 | 54.5 | 0.7761 | 0.0092 | 0.001835 | 2007 |
| SR-191 | 0.536 | 0.002 | 0 | 24.2 | 2.2149 | 0.0083 | 0 | 2007 |
| SR-192 | 0.144 | 0 | 0 | 10.9 | 1.3211 | 0 | 0 | 2007 |
| SR-193 | 0.091 | 0 | 0 | 17.3 | 0.5260 | 0 | 0 | 2007 |

Table A-1 Longitudinal Joint Cracking on the State Routes of Tennessee (Cont'd)

| State Route | Total Damage (mile) | | | Center-Line Length (mile) | Cracking Percentage | | | Year |
|---|---|---|---|---|---|---|---|---|
| | Low | Moderate | High | | Low | Moderate | High | |
| SR-194 | 0.123 | 0.002 | 0 | 23.1 | 0.5325 | 0.0087 | 0 | 2007 |
| SR-195 | 1.403 | 0.008 | 0 | 7.7 | 18.2208 | 0.1039 | 0 | 2007 |
| SR-196 | 0.116 | 0.002 | 0.001 | 25.7 | 0.4514 | 0.0078 | 0.0039 | 2007 |
| SR-197 | 0.029 | 0.002 | 0 | 12.6 | 0.2302 | 0.0159 | 0 | 2007 |
| SR-198 | 0.043 | 0 | 0 | 13.4 | 0.3209 | 0 | 0 | 2007 |
| SR-199 | 0.164 | 0.003 | 0 | 12.6 | 1.3016 | 0.0238 | 0 | 2007 |
| SR-200 | 0.063 | 0 | 0 | 22.1 | 0.2851 | 0 | 0 | 2007 |
| SR-201 | 0.047 | 0 | 0 | 16.4 | 0.2866 | 0 | 0 | 2007 |
| SR-202 | 0.48 | 0.001 | 0 | 16.5 | 2.9091 | 0.0061 | 0 | 2007 |
| SR-203 | 0.132 | 0 | 0 | 32.9 | 0.4012 | 0 | 0 | 2007 |
| SR-204 | 0.517 | 0 | 0 | 11.2 | 4.6161 | 0 | 0 | 2007 |
| SR-205 | 0.165 | 0.005 | 0 | 23.6 | 0.6992 | 0.0212 | 0 | 2007 |
| SR-206 | 0.005 | 0 | 0 | 7.7 | 0.0649 | 0 | 0 | 2007 |
| SR-207 | 0.001 | 0 | 0 | 1.1 | 0.0909 | 0 | 0 | 2007 |
| SR-208 | 0.033 | 0 | 0 | 1.5 | 2.2000 | 0 | 0 | 2007 |
| SR-209 | 0.339 | 0.009 | 0 | 17.2 | 1.9709 | 0.0523 | 0 | 2007 |
| SR-210 | 0.203 | 0.028 | 0 | 10.4 | 1.9519 | 0.2692 | 0 | 2007 |
| SR-211 | 0.651 | 0.019 | 0.014 | 17.1 | 3.8070 | 0.1111 | 0.0819 | 2007 |
| SR-212 | 0.018 | 0 | 0 | 2.5 | 0.7200 | 0 | 0 | 2007 |
| SR-214 | 1.789 | 0 | 0 | 8 | 22.3625 | 0 | 0 | 2007 |
| SR-215 | 0.002 | 0 | 0 | 2.1 | 0.0952 | 0 | 0 | 2007 |
| SR-216 | 0.446 | 0 | 0.001 | 16.4 | 2.7195 | 0 | 0.0061 | 2007 |
| SR-217 | 0.029 | 0 | 0 | 2.6 | 1.1154 | 0 | 0 | 2007 |
| SR-218 | 0.774 | 0 | 0 | 17.7 | 4.3729 | 0 | 0 | 2007 |
| SR-219 | 0.002 | 0 | 0 | 4 | 0.0500 | 0 | 0 | 2007 |
| SR-220 | 0.048 | 0 | 0 | 15.7 | 0.3057 | 0 | 0 | 2007 |
| SR-221 | 0.002 | 0 | 0 | 7.5 | 0.0267 | 0 | 0 | 2007 |
| SR-222 | 0.099 | 0 | 0 | 13.7 | 0.7226 | 0 | 0 | 2007 |
| SR-223 | 0.229 | 0.014 | 0 | 15.1 | 1.5166 | 0.0927 | 0 | 2007 |
| SR-224 | 0.393 | 0.015 | 0 | 25.5 | 1.5412 | 0.0588 | 0 | 2007 |
| SR-225 | 0.129 | 0.022 | 0.001 | 17.2 | 0.7500 | 0.1279 | 0.0058 | 2007 |
| SR-226 | 0.027 | 0 | 0 | 6.9 | 0.3913 | 0 | 0 | 2007 |
| SR-227 | 0.199 | 0 | 0 | 27.6 | 0.7210 | 0 | 0 | 2007 |
| SR-228 | 0.116 | 0 | 0 | 11.1 | 1.0450 | 0 | 0 | 2007 |
| SR-229 | 0.018 | 0 | 0 | 1.9 | 0.9474 | 0 | 0 | 2007 |

Table A-1 Longitudinal Joint Cracking on the State Routes of Tennessee (Cont'd)

| State Route | Total Damage (mile) | | | Center-Line Length (mile) | Cracking Percentage | | | Year |
|---|---|---|---|---|---|---|---|---|
| | Low | Moderate | High | | Low | Moderate | High | |
| SR-230 | 0.146 | 0.002 | 0 | 34.6 | 0.4220 | 0.0058 | 0 | 2007 |
| SR-231 | 0.019 | 0 | 0 | 13.8 | 0.1377 | 0 | 0 | 2007 |
| SR-232 | 0.113 | 0 | 0 | 13.7 | 0.8248 | 0 | 0 | 2007 |
| SR-233 | 0.003 | 0 | 0 | 21.2 | 0.0142 | 0 | 0 | 2007 |
| SR-234 | 0.157 | 0.024 | 0 | 6.8 | 2.3088 | 0.3529 | 0 | 2007 |
| SR-235 | 0.466 | 0 | 0 | 21 | 2.2190 | 0 | 0 | 2007 |
| SR-238 | 0.032 | 0.001 | 0 | 8.3 | 0.3855 | 0.0120 | 0 | 2007 |
| SR-239 | 0.039 | 0 | 0 | 0.8 | 4.8750 | 0 | 0 | 2007 |
| SR-243 | 0.04 | 0 | 0 | 12 | 0.3333 | 0 | 0 | 2007 |
| SR-245 | 0.02 | 0 | 0 | 18.7 | 0.1070 | 0 | 0 | 2007 |
| SR-246 | 0.033 | 0 | 0 | 21.8 | 0.1514 | 0 | 0 | 2007 |
| SR-247 | 0.09 | 0.001 | 0 | 24.9 | 0.3614 | 0.0040 | 0 | 2007 |
| SR-249 | 0.046 | 0 | 0 | 26.1 | 0.1762 | 0 | 0 | 2007 |
| SR-250 | 0.021 | 0 | 0 | 14 | 0.1500 | 0 | 0 | 2007 |
| SR-251 | 0.555 | 0.001 | 0 | 15.8 | 3.5127 | 0.0063 | 0 | 2007 |
| SR-252 | 0.119 | 0 | 0 | 13.4 | 0.8881 | 0 | 0 | 2007 |
| SR-253 | 0.012 | 0 | 0 | 7.4 | 0.1622 | 0 | 0 | 2007 |
| SR-254 | 0.103 | 0 | 0 | 17.3 | 0.5954 | 0 | 0 | 2007 |
| SR-255 | 0.077 | 0 | 0 | 11.1 | 0.6937 | 0 | 0 | 2007 |
| SR-256 | 0.059 | 0.001 | 0 | 10.7 | 0.5514 | 0.0093 | 0 | 2007 |
| SR-257 | 0.099 | 0.001 | 0 | 18.4 | 0.5380 | 0.0054 | 0 | 2007 |
| SR-258 | 0.012 | 0 | 0 | 14.2 | 0.0845 | 0 | 0 | 2007 |
| SR-259 | 0.004 | 0 | 0 | 12.9 | 0.0310 | 0 | 0 | 2007 |
| SR-260 | 0.007 | 0 | 0 | 5.7 | 0.1228 | 0 | 0 | 2007 |
| SR-261 | 0.017 | 0 | 0 | 13.5 | 0.1259 | 0 | 0 | 2007 |
| SR-262 | 0.008 | 0 | 0 | 10.6 | 0.0755 | 0 | 0 | 2007 |
| SR-263 | 0.001 | 0 | 0 | 5.2 | 0.0192 | 0 | 0 | 2007 |
| SR-264 | 0.002 | 0 | 0 | 9.9 | 0.0202 | 0 | 0 | 2007 |
| SR-265 | 0.071 | 0 | 0 | 24.9 | 0.2851 | 0 | 0 | 2007 |
| SR-266 | 0.053 | 0.002 | 0 | 39.9 | 0.1328 | 0.0050 | 0 | 2007 |
| SR-268 | 0.029 | 0 | 0 | 7.4 | 0.3919 | 0 | 0 | 2007 |
| SR-269 | 0.03 | 0.004 | 0 | 39.9 | 0.0752 | 0.0100 | 0 | 2007 |
| SR-270 | 0.009 | 0 | 0 | 9.5 | 0.0947 | 0 | 0 | 2007 |
| SR-272 | 0.007 | 0.001 | 0 | 20.4 | 0.0343 | 0.0049 | 0 | 2007 |
| SR-273 | 0.173 | 0.002 | 0 | 34.5 | 0.5014 | 0.0058 | 0 | 2007 |

Table A-1 Longitudinal Joint Cracking on the State Routes of Tennessee (Cont'd)

| State Route | Total Damage (mile) | | | Center-Line Length (mile) | Cracking Percentage | | | Year |
|---|---|---|---|---|---|---|---|---|
| | Low | Moderate | High | | Low | Moderate | High | |
| SR-275 | 0.005 | 0.001 | 0 | 14.2 | 0.0352 | 0.0070 | 0 | 2007 |
| SR-276 | 0.006 | 0 | 0 | 3.3 | 0.1818 | 0 | 0 | 2007 |
| SR-277 | 0.026 | 0 | 0 | 2.5 | 1.0400 | 0 | 0 | 2007 |
| SR-278 | 0.126 | 0.007 | 0.001 | 1.8 | 7.0000 | 0.3889 | 0.0556 | 2007 |
| SR-356 | 0.215 | 0.001 | 0 | 1 | 21.5000 | 0.1000 | 0 | 2007 |
| SR-364 | 0.07 | 0 | 0 | 3.3 | 2.1212 | 0 | 0 | 2007 |
| SR-365 | 0.307 | 0 | 0 | 3.6 | 8.5278 | 0 | 0 | 2007 |
| SR-366 | 0.121 | 0.003 | 0 | 6 | 2.0167 | 0.0500 | 0 | 2007 |
| SR-367 | 0.159 | 0 | 0 | 4.8 | 3.3125 | 0 | 0 | 2007 |
| SR-369 | 0.141 | 0 | 0 | 1.2 | 11.7500 | 0 | 0 | 2007 |
| SR-371 | 0.1 | 0.001 | 0.001 | 4.9 | 2.0408 | 0.0204 | 0.0204 | 2007 |
| SR-372 | 0.364 | 0.003 | 0 | 5.1 | 7.1373 | 0.0588 | 0 | 2007 |
| SR-373 | 0.408 | 0 | 0 | 17.3 | 2.3584 | 0 | 0 | 2007 |
| SR-374 | 0.031 | 0.001 | 0 | 16.2 | 0.1914 | 0.0062 | 0 | 2007 |
| SR-384 | 0.013 | 0.003 | 0 | 9.8 | 0.1327 | 0.0306 | 0 | 2007 |
| SR-386 | 0.019 | 0.001 | 0 | 9.6 | 0.1979 | 0.0104 | 0 | 2007 |
| SR-387 | 0.017 | 0 | 0 | 1.6 | 1.0625 | 0 | 0 | 2007 |
| SR-388 | 0.203 | 0 | 0 | 6.9 | 2.9420 | 0 | 0 | 2007 |
| SR-391 | 0.558 | 0.009 | 0.001 | 5.4 | 10.3333 | 0.1667 | 0.0185 | 2007 |
| SR-397 | 0.003 | 0.002 | 0 | 7.4 | 0.0405 | 0.0270 | 0 | 2007 |
| SR-417 | 0.001 | 0 | 0 | 1.9 | 0.0526 | 0 | 0 | 2007 |
| SR-420 | 0.002 | 0 | 0 | 4.6 | 0.0435 | 0 | 0 | 2007 |
| SR-421 | 0.006 | 0 | 0 | 5.6 | 0.1071 | 0 | 0 | 2007 |
| SR-423 | 0.412 | 0 | 0 | 10.8 | 3.8148 | 0 | 0 | 2007 |
| SR-424 | 0.058 | 0.002 | 0 | 17.2 | 0.3372 | 0.0116 | 0 | 2007 |
| SR-431 | 0.37 | 0.005 | 0 | 16.7 | 2.2156 | 0.0299 | 0 | 2007 |
| SR-436 | 0.042 | 0.001 | 0 | 9.8 | 0.4286 | 0.0102 | 0 | 2007 |
| SR-438 | 0.037 | 0 | 0.001 | 38.9 | 0.0951 | 0 | 0.0026 | 2007 |
| SR-441 | 0.003 | 0 | 0 | 3.7 | 0.0811 | 0 | 0 | 2007 |
| SR-445 | 1.054 | 0.043 | 0 | 12.7 | 8.2992 | 0.3386 | 0 | 2007 |
| SR-452 | 0.001 | 0 | 0 | 4.7 | 0.0213 | 0 | 0 | 2007 |
| SR-455 | 0.004 | 0 | 0 | 2 | 0.2000 | 0 | 0 | 2007 |
| SR-457 | 0.036 | 0 | 0 | 4.1 | 0.8780 | 0 | 0 | 2007 |
| SR-461 | 0.001 | 0 | 0 | 3 | 0.0333 | 0 | 0 | 2007 |
| SR-840 | 0.005 | 0 | 0 | 57.8 | 0.0087 | 0 | 0 | 2007 |

Table A-1 Longitudinal Joint Cracking on the State Routes of Tennessee (Cont'd)

| State Route | Total Damage (mile) | | | Center-Line Length (mile) | Cracking Percentage | | | Year |
|---|---|---|---|---|---|---|---|---|
| | Low | Moderate | High | | Low | Moderate | High | |
| SR-8 | 0.482 | 0.137 | 0.002 | 72.3 | 0.6667 | 0.1895 | 0.0028 | 2006 |
| SR-9 | 1.205 | 0.382 | 0.01 | 117.1 | 1.0290 | 0.3262 | 0.0085 | 2006 |
| SR-17 | 0.07 | 0 | 0 | 8.9 | 0.7865 | 0 | 0 | 2006 |
| SR-27 | 0.124 | 0.001 | 0.002 | 35.9 | 0.3454 | 0.0028 | 0.0056 | 2006 |
| SR-29 | 0.307 | 0.015 | 0 | 131.4 | 0.2336 | 0.0114 | 0 | 2006 |
| SR-30 | 0.43 | 0.037 | 0.003 | 115.9 | 0.3710 | 0.0319 | 0.0026 | 2006 |
| SR-31 | 0.005 | 0.003 | 0 | 17 | 0.0294 | 0.0176 | 0 | 2006 |
| SR-32 | 0.252 | 0.144 | 0.008 | 85.1 | 0.2961 | 0.1692 | 0.0094 | 2006 |
| SR-33 | 1.971 | 0.392 | 0.007 | 162.2 | 1.2152 | 0.2417 | 0.0043 | 2006 |
| SR-35 | 0.565 | 0.186 | 0.003 | 77 | 0.7338 | 0.2416 | 0.0039 | 2006 |
| SR-36 | 0.301 | 0.242 | 0.001 | 28.7 | 1.0488 | 0.8432 | 0.0035 | 2006 |
| SR-37 | 0.226 | 0.048 | 0.004 | 30.9 | 0.7314 | 0.1553 | 0.0129 | 2006 |
| SR-39 | 0.01 | 0 | 0 | 23.8 | 0.0420 | 0 | 0 | 2006 |
| SR-40 | 0.244 | 0.014 | 0 | 39.8 | 0.6131 | 0.0352 | 0 | 2006 |
| SR-44 | 0.152 | 0.077 | 0.001 | 17.1 | 0.8889 | 0.4503 | 0.0058 | 2006 |
| SR-58 | 0.39 | 0.002 | 0 | 81.9 | 0.4762 | 0.0024 | 0 | 2006 |
| SR-60 | 0.715 | 0.056 | 0.003 | 40.4 | 1.7698 | 0.1386 | 0.0074 | 2006 |
| SR-61 | 0.055 | 0.046 | 0.001 | 68.1 | 0.0808 | 0.0675 | 0.0015 | 2006 |
| SR-62 | 0.057 | 0.004 | 0 | 82.5 | 0.0691 | 0.0048 | 0 | 2006 |
| SR-63 | 0.603 | 0.184 | 0 | 86.6 | 0.6963 | 0.2125 | 0 | 2006 |
| SR-66 | 0.043 | 0.013 | 0.002 | 60.2 | 0.0714 | 0.0216 | 0.0033 | 2006 |
| SR-67 | 0.028 | 0.002 | 0 | 48.5 | 0.0577 | 0.0041 | 0 | 2006 |
| SR-68 | 0.061 | 0.026 | 0 | 104.4 | 0.0584 | 0.0249 | 0 | 2006 |
| SR-70 | 0.088 | 0.096 | 0.009 | 58.3 | 0.1509 | 0.1647 | 0.0154 | 2006 |
| SR-71 | 0.368 | 0.145 | 0.002 | 60.5 | 0.6083 | 0.2397 | 0.0033 | 2006 |
| SR-72 | 0.023 | 0.001 | 0 | 38.2 | 0.0602 | 0.0026 | 0 | 2006 |
| SR-73 | 0.235 | 0.096 | 0.006 | 87 | 0.2701 | 0.1103 | 0.0069 | 2006 |
| SR-74 | 0.034 | 0.001 | 0 | 17.5 | 0.1943 | 0.0057 | 0 | 2006 |
| SR-75 | 0.031 | 0.019 | 0.003 | 27.7 | 0.1119 | 0.0686 | 0.0108 | 2006 |
| SR-81 | 0.176 | 0.003 | 0 | 25.6 | 0.6875 | 0.0117 | 0 | 2006 |
| SR-83 | 0.011 | 0 | 0 | 7.8 | 0.1410 | 0 | 0 | 2006 |
| SR-84 | 0.352 | 0 | 0 | 38.6 | 0.9119 | 0 | 0 | 2006 |
| SR-90 | 0.004 | 0 | 0 | 13.5 | 0.0296 | 0 | 0 | 2006 |
| SR-91 | 0.064 | 0.011 | 0 | 40.7 | 0.1572 | 0.0270 | 0 | 2006 |
| SR-92 | 0.002 | 0.001 | 0 | 33.1 | 0.0060 | 0.0030 | 0 | 2006 |

Table A-1 Longitudinal Joint Cracking on the State Routes of Tennessee (Cont'd)

| State Route | Total Damage (mile) | | | Center-Line Length (mile) | Cracking Percentage | | | Year |
|---|---|---|---|---|---|---|---|---|
| | Low | Moderate | High | | Low | Moderate | High | |
| SR-93 | 0.073 | 0.059 | 0 | 38.4 | 0.1901 | 0.1536 | 0 | 2006 |
| SR-95 | 0.01 | 0.003 | 0 | 29.6 | 0.0338 | 0.0101 | 0 | 2006 |
| SR-101 | 0.04 | 0.001 | 0 | 32.9 | 0.1216 | 0.0030 | 0 | 2006 |
| SR-107 | 0.758 | 0.085 | 0.001 | 56.3 | 1.3464 | 0.1510 | 0.0018 | 2006 |
| SR-108 | 0.095 | 0 | 0 | 53.7 | 0.1769 | 0 | 0 | 2006 |
| SR-111 | 0.143 | 0.065 | 0 | 105.6 | 0.1354 | 0.0616 | 0 | 2006 |
| SR-115 | 0.416 | 0.029 | 0.003 | 48.7 | 0.8542 | 0.0595 | 0.0062 | 2006 |
| SR-116 | 0.015 | 0.013 | 0.002 | 21.4 | 0.0701 | 0.0607 | 0.0093 | 2006 |
| SR-123 | 0.001 | 0 | 0 | 1.3 | 0.0769 | 0 | 0 | 2006 |
| SR-127 | 0.047 | 0 | 0 | 34.7 | 0.1354 | 0 | 0 | 2006 |
| SR-131 | 0.171 | 0.075 | 0 | 42.3 | 0.4043 | 0.1773 | 0 | 2006 |
| SR-133 | 0.002 | 0 | 0 | 11.4 | 0.0175 | 0 | 0 | 2006 |
| SR-134 | 0.045 | 0.001 | 0 | 6.5 | 0.6923 | 0.0154 | 0 | 2006 |
| SR-135 | 0.129 | 0.313 | 0.001 | 56 | 0.2304 | 0.5589 | 0.0018 | 2006 |
| SR-136 | 0.213 | 0.006 | 0 | 52.5 | 0.4057 | 0.0114 | 0 | 2006 |
| SR-137 | 0.001 | 0.002 | 0 | 3 | 0.0333 | 0.0667 | 0 | 2006 |
| SR-139 | 0.128 | 0.007 | 0 | 23.3 | 0.5494 | 0.0300 | 0 | 2006 |
| SR-143 | 0.068 | 0.056 | 0.006 | 12.6 | 0.5397 | 0.4444 | 0.0476 | 2006 |
| SR-144 | 0.001 | 0.02 | 0.002 | 7.6 | 0.0132 | 0.2632 | 0.0263 | 2006 |
| SR-145 | 0.006 | 0 | 0 | 9.6 | 0.0625 | 0 | 0 | 2006 |
| SR-146 | 0.017 | 0.001 | 0 | 17.6 | 0.0966 | 0.0057 | 0 | 2006 |
| SR-148 | 0.008 | 0 | 0 | 3.9 | 0.2051 | 0 | 0 | 2006 |
| SR-150 | 0.004 | 0 | 0 | 16.7 | 0.0240 | 0 | 0 | 2006 |
| SR-153 | 0.003 | 0 | 0 | 12.8 | 0.0234 | 0 | 0 | 2006 |
| SR-154 | 0.09 | 0 | 0 | 19.5 | 0.4615 | 0 | 0 | 2006 |
| SR-156 | 0.129 | 0 | 0 | 35.3 | 0.3654 | 0 | 0 | 2006 |
| SR-158 | 0.02 | 0.007 | 0 | 4.4 | 0.4545 | 0.1591 | 0 | 2006 |
| SR-159 | 0.008 | 0.008 | 0 | 12.4 | 0.0645 | 0.0645 | 0 | 2006 |
| SR-160 | 0.012 | 0.011 | 0.013 | 27.1 | 0.0443 | 0.0406 | 0.0480 | 2006 |
| SR-162 | 0.001 | 0.001 | 0 | 5.9 | 0.0169 | 0.0169 | 0 | 2006 |
| SR-163 | 0.01 | 0 | 0 | 15.4 | 0.0649 | 0 | 0 | 2006 |
| SR-164 | 0.011 | 0.01 | 0 | 16.8 | 0.0655 | 0.0595 | 0 | 2006 |
| SR-165 | 0.003 | 0 | 0 | 23.8 | 0.0126 | 0 | 0 | 2006 |
| SR-167 | 0.166 | 0.021 | 0 | 20.9 | 0.7943 | 0.1005 | 0 | 2006 |
| SR-169 | 0.008 | 0 | 0 | 11.5 | 0.0696 | 0 | 0 | 2006 |

Table A-1 Longitudinal Joint Cracking on the State Routes of Tennessee (Cont'd)

| State Route | Total Damage (mile) | | | Center-Line Length (mile) | Cracking Percentage | | | Year |
|---|---|---|---|---|---|---|---|---|
| | Low | Moderate | High | | Low | Moderate | High | |
| SR-170 | 0.049 | 0.011 | 0 | 34.1 | 0.1437 | 0.0323 | 0 | 2006 |
| SR-173 | 0.023 | 0.005 | 0 | 7.3 | 0.3151 | 0.0685 | 0 | 2006 |
| SR-279 | 0.001 | 0 | 0 | 5.3 | 0.0189 | 0 | 0 | 2006 |
| SR-280 | 0.001 | 0 | 0 | 10.6 | 0.0094 | 0 | 0 | 2006 |
| SR-281 | 0.007 | 0 | 0 | 6 | 0.1167 | 0 | 0 | 2006 |
| SR-283 | 0.199 | 0.032 | 0.001 | 13.6 | 1.4632 | 0.2353 | 0.0074 | 2006 |
| SR-284 | 0.007 | 0.004 | 0 | 15.2 | 0.0461 | 0.0263 | 0 | 2006 |
| SR-285 | 0.099 | 0.004 | 0.001 | 22 | 0.4500 | 0.0182 | 0.0045 | 2006 |
| SR-286 | 0.098 | 0.001 | 0 | 2.8 | 3.5000 | 0.0357 | 0 | 2006 |
| SR-287 | 0.031 | 0.001 | 0 | 40.3 | 0.0769 | 0.0025 | 0 | 2006 |
| SR-288 | 0.056 | 0 | 0 | 17.8 | 0.3146 | 0 | 0 | 2006 |
| SR-289 | 0.005 | 0 | 0 | 2.6 | 0.1923 | 0 | 0 | 2006 |
| SR-290 | 0.006 | 0.073 | 0 | 18.9 | 0.0317 | 0.3862 | 0 | 2006 |
| SR-291 | 0.016 | 0.032 | 0 | 2 | 0.8000 | 1.6000 | 0 | 2006 |
| SR-292 | 0.007 | 0.001 | 0 | 9.8 | 0.0714 | 0.0102 | 0 | 2006 |
| SR-293 | 0.004 | 0 | 0 | 11.2 | 0.0357 | 0 | 0 | 2006 |
| SR-294 | 0.072 | 0 | 0 | 16.4 | 0.4390 | 0 | 0 | 2006 |
| SR-296 | 0.001 | 0 | 0 | 3 | 0.0333 | 0 | 0 | 2006 |
| SR-297 | 0.11 | 0.016 | 0.001 | 40.9 | 0.2689 | 0.0391 | 0.0024 | 2006 |
| SR-298 | 0.007 | 0 | 0 | 25.8 | 0.0271 | 0 | 0 | 2006 |
| SR-299 | 0.019 | 0.004 | 0.001 | 15.4 | 0.1234 | 0.0260 | 0.0065 | 2006 |
| SR-301 | 0.001 | 0 | 0 | 0.9 | 0.1111 | 0 | 0 | 2006 |
| SR-302 | 0.001 | 0 | 0 | 12.2 | 0.0082 | 0 | 0 | 2006 |
| SR-303 | 0.033 | 0 | 0 | 5.7 | 0.5789 | 0 | 0 | 2006 |
| SR-304 | 0.007 | 0 | 0 | 29.4 | 0.0238 | 0 | 0 | 2006 |
| SR-305 | 0.004 | 0 | 0.003 | 13.6 | 0.0294 | 0 | 0.0221 | 2006 |
| SR-306 | 0.021 | 0 | 0 | 11.1 | 0.1892 | 0 | 0 | 2006 |
| SR-307 | 0.004 | 0.001 | 0 | 10.8 | 0.0370 | 0.0093 | 0 | 2006 |
| SR-308 | 0.001 | 0 | 0 | 7.5 | 0.0133 | 0 | 0 | 2006 |
| SR-310 | 0.001 | 0 | 0 | 6.2 | 0.0161 | 0 | 0 | 2006 |
| SR-311 | 0.007 | 0 | 0 | 6 | 0.1167 | 0 | 0 | 2006 |
| SR-312 | 0.015 | 0 | 0 | 26.2 | 0.0573 | 0 | 0 | 2006 |
| SR-313 | 0.056 | 0 | 0 | 7.8 | 0.7179 | 0 | 0 | 2006 |
| SR-314 | 0.14 | 0 | 0 | 6 | 2.3333 | 0 | 0 | 2006 |
| SR-317 | 0.287 | 0.002 | 0 | 20.8 | 1.3798 | 0.0096 | 0 | 2006 |

Table A-1 Longitudinal Joint Cracking on the State Routes of Tennessee (Cont'd)

| State Route | Total Damage (mile) | | | Center-Line Length (mile) | Cracking Percentage | | | Year |
|---|---|---|---|---|---|---|---|---|
| | Low | Moderate | High | | Low | Moderate | High | |
| SR-318 | 0.001 | 0 | 0 | 1 | 0.1000 | 0 | 0 | 2006 |
| SR-319 | 0.052 | 0.001 | 0 | 21.3 | 0.2441 | 0.0047 | 0 | 2006 |
| SR-320 | 0.111 | 0 | 0 | 7.3 | 1.5205 | 0 | 0 | 2006 |
| SR-321 | 0.009 | 0 | 0 | 7.1 | 0.1268 | 0 | 0 | 2006 |
| SR-322 | 0.039 | 0 | 0 | 25.6 | 0.1523 | 0 | 0 | 2006 |
| SR-325 | 0.004 | 0.001 | 0 | 15.5 | 0.0258 | 0.0065 | 0 | 2006 |
| SR-326 | 0.002 | 0 | 0 | 1.3 | 0.1538 | 0 | 0 | 2006 |
| SR-330 | 0.005 | 0.001 | 0 | 9.1 | 0.0549 | 0.0110 | 0 | 2006 |
| SR-331 | 0.007 | 0 | 0 | 16 | 0.0438 | 0 | 0 | 2006 |
| SR-332 | 0.057 | 0.007 | 0 | 14.2 | 0.4014 | 0.0493 | 0 | 2006 |
| SR-333 | 0.027 | 0.002 | 0 | 14.5 | 0.1862 | 0.0138 | 0 | 2006 |
| SR-334 | 0.001 | 0 | 0.001 | 2.5 | 0.0400 | 0 | 0.0400 | 2006 |
| SR-335 | 0.077 | 0.001 | 0 | 10.4 | 0.7404 | 0.0096 | 0 | 2006 |
| SR-336 | 0.01 | 0.003 | 0.001 | 19.6 | 0.0510 | 0.0153 | 0.0051 | 2006 |
| SR-337 | 0.003 | 0.001 | 0 | 1.5 | 0.2000 | 0.0667 | 0 | 2006 |
| SR-338 | 0.009 | 0.007 | 0 | 18.6 | 0.0484 | 0.0376 | 0 | 2006 |
| SR-339 | 0.004 | 0.004 | 0 | 16.9 | 0.0237 | 0.0237 | 0 | 2006 |
| SR-340 | 0.015 | 0.017 | 0.003 | 25.5 | 0.0588 | 0.0667 | 0.0118 | 2006 |
| SR-341 | 0.074 | 0 | 0 | 10.4 | 0.7115 | 0 | 0 | 2006 |
| SR-342 | 0.038 | 0.039 | 0 | 4.4 | 0.8636 | 0.8864 | 0 | 2006 |
| SR-343 | 0.009 | 0.019 | 0.003 | 7.4 | 0.1216 | 0.2568 | 0.0405 | 2006 |
| SR-344 | 0.002 | 0.003 | 0.001 | 9.8 | 0.0204 | 0.0306 | 0.0102 | 2006 |
| SR-345 | 0.004 | 0.001 | 0 | 8.5 | 0.0471 | 0.0118 | 0 | 2006 |
| SR-346 | 0.222 | 0.035 | 0 | 19.7 | 1.1269 | 0.1777 | 0 | 2006 |
| SR-347 | 0.007 | 0.005 | 0.001 | 20.8 | 0.0337 | 0.0240 | 0.0048 | 2006 |
| SR-348 | 0 | 0.001 | 0.001 | 12 | 0.0000 | 0.0083 | 0.0083 | 2006 |
| SR-349 | 0.001 | 0.001 | 0 | 13.2 | 0.0076 | 0.0076 | 0 | 2006 |
| SR-350 | 0.021 | 0.024 | 0 | 7 | 0.3000 | 0.3429 | 0 | 2006 |
| SR-351 | 0.166 | 0.037 | 0 | 23.1 | 0.7186 | 0.1602 | 0 | 2006 |
| SR-352 | 0.019 | 0.016 | 0 | 9 | 0.2111 | 0.1778 | 0 | 2006 |
| SR-354 | 0.005 | 0 | 0 | 7.4 | 0.0676 | 0 | 0 | 2006 |
| SR-357 | 0 | 0.002 | 0 | 2.4 | 0.0000 | 0.0833 | 0 | 2006 |
| SR-358 | 0.042 | 0.038 | 0.004 | 9.4 | 0.4468 | 0.4043 | 0.0426 | 2006 |
| SR-359 | 0.046 | 0.024 | 0 | 4.8 | 0.9583 | 0.5000 | 0 | 2006 |
| SR-360 | 0.034 | 0 | 0 | 22.1 | 0.1538 | 0 | 0 | 2006 |

Table A-1 Longitudinal Joint Cracking on the State Routes of Tennessee (Cont'd)

| State Route | Total Damage (mile) | | | Center-Line Length (mile) | Cracking Percentage | | | Year |
|---|---|---|---|---|---|---|---|---|
| | Low | Moderate | High | | Low | Moderate | High | |
| SR-361 | 0.011 | 0.004 | 0.001 | 8.8 | 0.1250 | 0.0455 | 0.0114 | 2006 |
| SR-362 | 0.026 | 0.019 | 0.002 | 5.9 | 0.4407 | 0.3220 | 0.0339 | 2006 |
| SR-363 | 0.009 | 0 | 0 | 6 | 0.1500 | 0 | 0 | 2006 |
| SR-370 | 0.068 | 0.004 | 0 | 5.7 | 1.1930 | 0.0702 | 0 | 2006 |
| SR-375 | 0.217 | 0.004 | 0 | 18.2 | 1.1923 | 0.0220 | 0 | 2006 |
| SR-378 | 0.001 | 0 | 0 | 1.7 | 0.0588 | 0 | 0 | 2006 |
| SR-380 | 0.006 | 0 | 0.001 | 4.7 | 0.1277 | 0 | 0.0213 | 2006 |
| SR-381 | 0.105 | 0 | 0 | 7.7 | 1.3636 | 0 | 0 | 2006 |
| SR-390 | 0.027 | 0.069 | 0.001 | 2.3 | 1.1739 | 3.0000 | 0.0435 | 2006 |
| SR-392 | 0.006 | 0.001 | 0 | 5.2 | 0.1154 | 0.0192 | 0 | 2006 |
| SR-394 | 0.035 | 0.086 | 0.002 | 15.6 | 0.2244 | 0.5513 | 0.0128 | 2006 |
| SR-395 | 0.005 | 0.013 | 0.001 | 6.1 | 0.0820 | 0.2131 | 0.0164 | 2006 |
| SR-399 | 0 | 0.004 | 0 | 10.6 | 0.0000 | 0.0377 | 0 | 2006 |
| SR-400 | 0.04 | 0.018 | 0 | 12.4 | 0.3226 | 0.1452 | 0 | 2006 |
| SR-416 | 0.016 | 0.01 | 0.007 | 14.6 | 0.1096 | 0.0685 | 0.0479 | 2006 |
| SR-419 | 0.002 | 0 | 0 | 4 | 0.0500 | 0 | 0 | 2006 |
| SR-422 | 0.001 | 0 | 0 | 2.3 | 0.0435 | 0 | 0 | 2006 |
| SR-429 | 0.216 | 0 | 0 | 1.8 | 12.0000 | 0 | 0 | 2006 |
| SR-433 | 0.007 | 0 | 0 | 8.3 | 0.0843 | 0 | 0 | 2006 |
| SR-435 | 0.006 | 0.002 | 0 | 4.1 | 0.1463 | 0.0488 | 0 | 2006 |
| SR-443 | 0.009 | 0 | 0 | 12.1 | 0.0744 | 0 | 0 | 2006 |
| SR-446 | 0.008 | 0 | 0 | 0.3 | 2.6667 | 0 | 0 | 2006 |
| SR-447 | 0.001 | 0.006 | 0.001 | 0.1 | 1.0000 | 6.0000 | 1.0000 | 2006 |
| SR-454 | 0.024 | 0.005 | 0.001 | 6.4 | 0.3750 | 0.0781 | 0.0156 | 2006 |
| SR-456 | 0.004 | 0 | 0 | 10 | 0.0400 | 0 | 0 | 2006 |